中国激光

激光诱导击穿光谱技术及应用综述

李祥友*，刘可，周冉，张闻

华中科技大学武汉光电国家研究中心，湖北，武汉 430074

摘要　元素的成分和含量对材料的性能起着至关重要的作用，常规的检测方法能够获取待测样品的类别和成分信息，但存在成本高、操作复杂、效率低等问题。应用领域的不断扩展对分析技术有了更高的需求，找寻一种更新、更快、适应性更强的检测技术成为当前的研究热点。激光诱导击穿光谱技术具有多元素同时检测、结构简单、检测速度快、不受样品形态影响等特点，在诸多领域展现出广阔的应用前景。基于此，综述了激光诱导击穿光谱技术的机理、装置类型、基础研究进展以及应用研究，并对其发展趋势进行了展望。

关键词　光谱学；激光诱导击穿光谱；机理；信号增强；定性定量分析；应用

中图分类号　O433　　　**文献标志码**　A　　　　　　　　　　**DOI**：10.3788/CJL202249.1202003

1　引　　言

材料的元素成分和含量决定着材料的物理和化学性能，快速、准确、低成本地获取材料的成分和含量信息一直是研究学者的努力方向。现有的成分分析方法可以分为化学分析法和仪器分析法。化学分析法以化学反应定律为基础，对样品的化学组成进行定性定量的系统分析，包括重量法、容量法和比色法等[1-3]。仪器分析法通过分析仪器直接获取待测样品的物理和化学信息，如电感耦合等离子体质谱（ICP-MS）[4-5]、拉曼光谱[6-7]、近红外光谱（NIR）[8-9]、X射线荧光光谱法（XRF）[10-11]和原子吸收光谱法（AAS）[12-13]等。上述分析方法可以获取待测样品的类别和成分信息，并具有较高的灵敏度和准确度，但存在操作复杂、成本高、效率低等问题。应用领域的不断扩展对分析技术有了更高的要求，找寻一种更新、更快、适应性更强的检测技术成为当前的研究热点。

激光诱导击穿光谱（LIBS）技术是一种极具发展潜力的元素分析技术[14-16]。它以激光作为激发源烧蚀待测样品产生等离子体，通过光谱仪探测等离子体的发射光谱，对光谱进行分析即可获得待测样品的元素类别和含量信息[17]。相对于其他分析技术，LIBS 技术具有多元素同时检测、结构简单、检测速度快、不受样品形态影响等独特优势[18-20]，在诸多领域展现出广阔的应用前景。基于此，本文综述了 LIBS 技术的机理、装置、基础研究进展以及应用研究，并对其发展趋势进行了展望。

2　LIBS 技术机理及装置

2.1　LIBS 技术机理

2.1.1　等离子体特性

研究等离子体的相关特性有助于理解激光诱导等离子体的产生机理、解决 LIBS 分析过程中遇到的相关难题并提高 LIBS 分析的精准度。

研究等离子体随时间的变化特性对于理解等离子体的产生、扩散和湮灭意义重大。Guo 等[21]研究发现，样品温度越高，时间分辨等离子体电子温度和电子数密度越高，电子数密度的衰减速度越快。Hansen 等[22]利用 LIBS 等离子体的静止模型，模拟火星大气条件下的时间分辨 LIBS。Kumar 等[23]利用时间分辨测量方法，估计了 Al 谐振线的斯塔克展宽系数。Hemalaxmi 等[24]利用时间分辨 LIBS，研究了煤激光烧蚀等离子体中碳原子（C I）和分子碳（CN 和 C_2）的来源、形成机理和持续时间。Wang 等[25]研究了火花放电辅助 fs-LIBS 在不同放电电压

和激光能量下的时间分辨光谱,发现使用火花放电可以显著提高光谱强度。

对于光谱技术来说,空间分辨率也是最关键的参数之一。Ghezelbash 等[26]采用 LIBS 技术记录了不同层流扩散甲醇、乙醇和正丙醇火焰的等离子体辐射,研究了不同区域燃烧的形状、结构、种类和质量。Li 等[27]测量了 ns-LIBS 在两种平行气体流边界处的一维光谱,发现 ns-LIBS 在气体中的空间分辨率是测量 LIBS 时等离子体的大小。Mal 等[28]利用空间分辨 LIBS 研究了 W 元素的激光诱导等离子体。Aragón 等[29]研究了单脉冲激光等离子体的强度空间分布。Corsi 等[30]研究了双脉冲激光等离子体的强度空间分布以及等离子体电子数密度和温度特性。Xiu 等[31-33]系统研究了氩气气氛下有机样品光谱的空间分布特性,发现光谱的空间分布具有特异性,会随着元素种类的改变而改变。

2.1.2 自吸收效应

等离子体之所以产生自吸收效应,是因为空间分布的等离子体的中心温度高,外围温度低,中心激发态原子发射的光子会被外围同类基态冷粒子吸收,谱线中心强度减弱甚至出现凹陷,从而影响光谱强度与相关元素浓度之间的线性关系,降低定量分析的准确度。

一些研究人员通过理论模型对自吸收因子进行了校正。Amamou 等[34]将洛伦兹线型和高斯线型假设为谱线线型,进而推导出相应的自吸收校正因子,研究发现,校正后计算所得的多重谱线的跃迁几率比值与理论值更接近。El Sherbini 等[35]采用自吸收系数评估和校正了均匀等离子体中的自吸收效应,并对比了不同延时下 Al 元素原子谱线和离子谱线的自吸收系数。

成长曲线法(COG)是通过光谱强度和等离子体光学厚度之间的映射关系来评估和校正自吸收效应的方法。Aguilera 等[36]利用 COG 分析了铁镍合金中 Fe 原子线和离子线的自吸收效应随时间变化的趋势,发现 Fe 原子谱线的自吸收随采集延时的增加而增强,而 Fe 离子线的自吸收基本不随采集延时变化。Aragón 等[37]从 COG 进一步推导出CSigma 图,通过吸收截面大小判断自吸收严重程度,吸收截面越大则自吸收越严重,因此只要已知元素的原子数据并且不超过有效性限制,即可预测特定浓度元素的给定谱线的强度和自吸收。

通过分析谱线与参考线谱线的比值关系对自吸收进行校正,能够减少激光能量波动对分析结果的影响。Bredice 等[38]利用谱线比值法对自吸收进行了校正,发现双脉冲的自吸收效应比单脉冲更为严重。Sun 等[39]通过内标校正自吸收效应,并利用校正后的谱线强度绘制 Boltzmann 曲线,获得了稳定的等离子体温度和校正结果。Hou 等[40]假设等离子体处于局部热力学平衡状态,通过同一元素相同电离态的两条谱线的比值与理论值的关系判断是否存在自吸收效应。

也有不少研究人员从实验的角度分析、校正 LIBS 中的自吸收效应。Chen 等[41]采用平面反射镜装置约束激光等离子体,提高了等离子体的温度和电子数密度,有效地降低了光谱的自吸收程度,并降低了 Mn 和 Ni 元素的相对标准偏差。Moon 等[42]利用反射镜法计算了自吸收校正因子,定标曲线的定标范围从 0.1% 扩展到 1.2%。Burger 等[43]通过反射镜法将 Cu II 240.33 nm 谱线的半峰全宽减小了 5%。Yi 等[44]为了降低土壤等离子体中 Na、K、Pb 和 Cu 元素的自吸收,采用空间分辨 LIBS 方法对土壤等离子体中 Na、K、Pb 和 Cu 元素进行了研究,结果表明,通过选择等离子体的采集区域,可大幅度降低 LIBS 的自吸收效应,显著提高 LIBS 的定量精度。Li 等[45-46]则发现,激光受激吸收效应对等离子体自吸收效应具有抑制效果,可利用波长可调谐的非聚焦激光辐照整个等离子体,大幅减小了等离子体外层冷原子的数量,从而有效抑制等离子体的自吸收效应(图 1)。Hao 等[47]研究发现,当气压降低至 1 kPa 时,激光诱导等离子体基本无自吸收(图 2),同时定标曲线的线性相关系数提升至 0.99 以上。

2.2 LIBS 装置

2.2.1 实验室 LIBS 装置

实验室 LIBS 装置具有光谱探测范围广、分辨率高、波动小等优点,检测灵敏度和重现性较好,常被用于机理研究和探索性应用研究。

合适的硬件系统和实验参数是 LIBS 测量的先决条件,需要依据分析需求仔细配置[48]。Fink 等[49]对比了不同波长(266 nm 和 1064 nm)的激光器对 96 种电子废弃回收粉碎物的烧蚀效果,实验结果表明,在 266 nm 激光器的作用下,光谱重现性更好。Wang 等[50]对比了红外和紫外激光器下 7 种塑料制品的等离子体烧蚀阈值和信噪比,结果表明,相对于紫外激光器,红外激光器激发样品产生的等离子体发射光谱信号更好,强度更高。Negre 等[51]获取了不同延时时间下的 LIBS 等离子体图像,并用不同的颜色标识了塑料样品内不同元素和分子的分
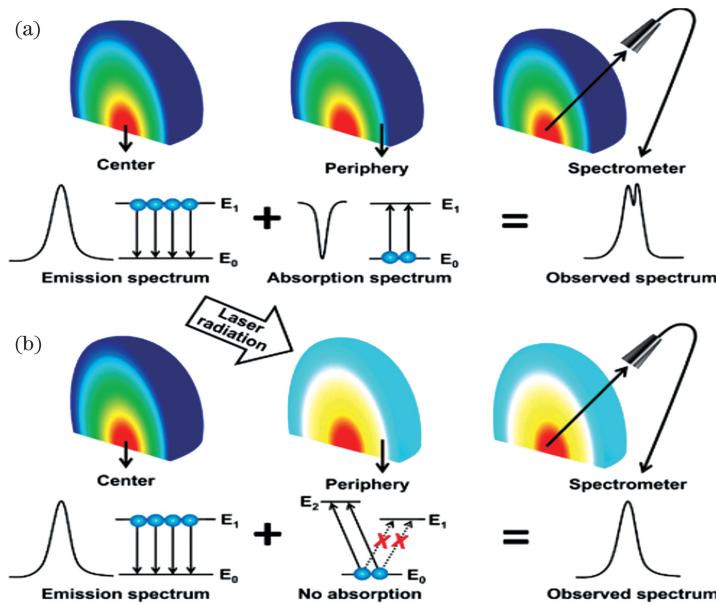
图 1 自吸收抑制原理示意图[45]。(a)LIBS 等离子体中的自吸收效应;(b)LIBS 等离子体中的受激吸收效应

Fig. 1 Schematics of self-absorption reduction[45]. (a) Self-absorption in LIBS plasma; (b) laser-stimulated absorption in LIBS plasma
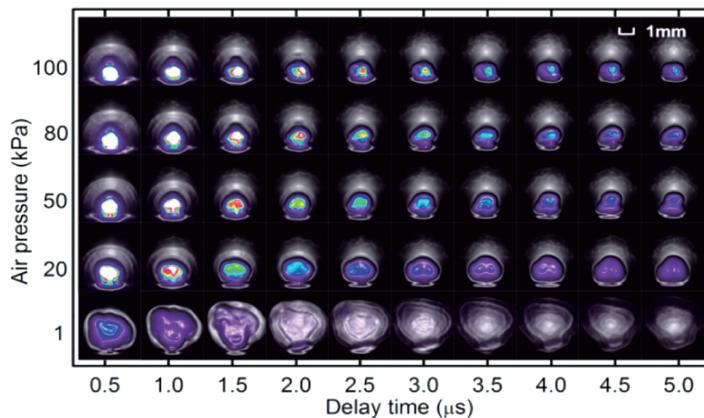

图 2 不同延时和空气压力下等离子体的图像[47]

Fig. 2 Images of plasma plumes under different delay time and air pressures[47]

布情况。Viskup 等[52]利用双脉冲 LIBS(DP-LIBS)装置对 9 种塑料样品进行了激发,并利用增强电荷耦合器件(ICCD)采集了不同延迟时间下的 LIBS 图像,结果表明,通过优化脉冲间隔可以提高光谱信号的强度和灵敏度,但最佳的参数与塑料基体类型和目标元素有关。

通过两种技术的互补性能够更好地区分不同类别的样品,但此种联用方式也增加了仪器成本。Moros 等[53-55]将 LIBS 技术与 Raman 光谱技术联用,实现了对爆炸物、分子、塑料等的分析,其原理如图 3 所示,有效克服了单一分析技术的局限性,显著提升了 LIBS 技术的适用性和有效性。Liu 等[56]根据等离子体边缘温度低的特点,使用微波对等离子体进行加热,提高了等离子体的外围温度,显著增
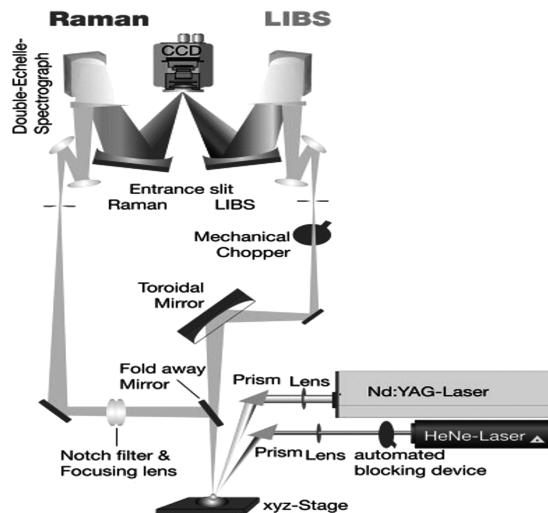

图 3 LIBS-Raman 装置[54]

Fig. 3 LIBS-Raman setup[54]

强了 Cu 和 Ag 元素的光谱信号，分别获得了 30 mg/kg 和 23.3 mg/kg 的检测极限。Jiang 等[57] 采用 LIBS 与电化学结合的方法检测水稻消解液中的 Cd 元素，检测极限可达 0.016 mg/kg。

2.2.2　远程 LIBS 装置

远程 LIBS 装置可以在保证人员安全的前提下，实现恶劣条件下或者危险品的原位稳定检测。

Liu 等[58-59] 将 LIBS 分析系统集成于磁约束受控核聚变托卡马克装置中，实现了对极端环境下样品的远距离元素分析。Sun 等[60] 为了实时在线监测钢铁冶炼过程中钢液成分的变化，研发了一套在钢厂恶劣环境下能稳定、可靠运行的远程 LIBS 系统。Guirado 等[61-62] 采用 532 nm 的 Nd∶YAG 激光器和望远镜光学系统成功搭建了移动式的远程 LIBS 系统，成功实现了对深海海下目标的近距离

（80 cm）分析，并研究了海水温度和水下光路对光谱信号的影响。为减小采集系统的体积和成本，Li 等[63] 设计了一套基于仿生复眼结构的多探头光谱收集装置，如图 4 所示，在保证采集效率的前提下，提高了定量分析性能。Homma 等[64] 利用远程 LIBS 装置实现了 10 m 距离以内检测户外高压输电线路的硅橡胶复合绝缘子，并对老化的复合绝缘子表面进行了深度剖面分析。Kokkinaki 等[65] 也搭建了远程 LIBS 装置并对距离 10 m 的老化聚合物绝缘体进行了分析，研究了聚合物复合材料类型的识别和其中 C、Si 元素含量，有效评估了老化绝缘体的物理状态。Junjuri 等[66] 研究了一台远程 LIBS 装置并对 6.5 m 外的爆炸物进行了识别，再结合二维散点图方法和主成分分析（PCA）法，对 5 种炸药和 19 种非炸药的识别率分别达到了 98% 和 94%。
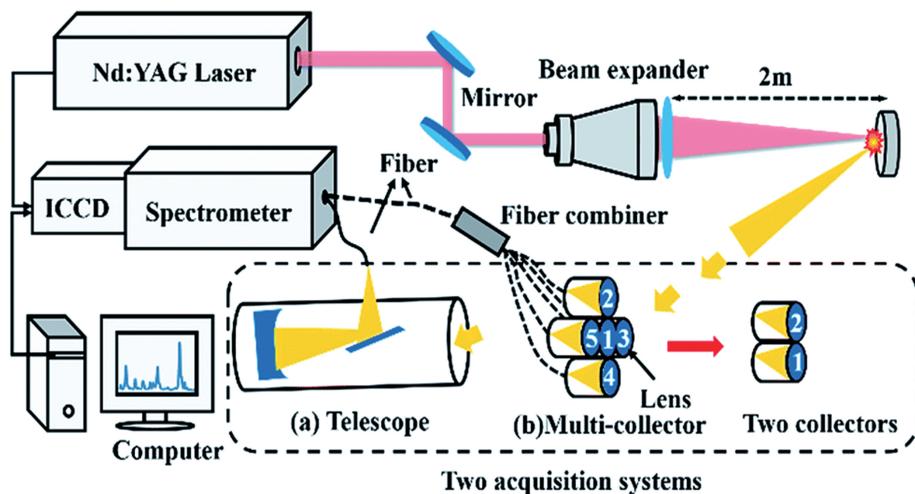

图 4　远程 LIBS 装置示意图[63]。(a)望远镜；(b)多探头系统

Fig. 4　Schematic of stand-off LIBS[63]. (a) Telescope; (b) multi-collector system

2.2.3　在线 LIBS 装置

由于 LIBS 技术具有原位、实时、快速、无需复杂样品预处理等独特优势，LIBS 装置能够快速处理生产线上的海量样品。但由于样品形态、表面脏污、环境改变等原因，在线 LIBS 装置的检测灵敏度一般低于实验室装置。

Gaft 等[67] 提出了利用 LIBS 在线分析传送带上大块矿石的新思路，该系统能够实现 MgO、Fe_2O_3、Al_2O_3 的半定量分析。Noll 等[68] 研制出一套用于在线检测炼钢厂炉渣中金属元素的自动化 LIBS 设备，该设备将一个长柄状的探针伸入 600～1400 ℃ 的炉渣中进行分析，可自动对其中的 CaO、Fe、SiO_2、MgO、Mn 和 Al_2O_3 等进行检测，单次测量仅需 2 min。同时，针对钢铁的生产控制和质量

保障，Noll 等[69] 开发了一系列 LIBS 分析装置，钢液中 Ni 定标曲线的决定系数（R^2）可达 0.9970，检测极限低至 8500 mg/kg，如图 5 所示。Zhang 等[70] 开发了一种自动原型 LIBS 装置，包括等速取样器、样品制备模块和 LIBS 模块，可用于发电厂在线分析飞灰中的未燃烧碳，而不受燃煤类型的影响。Redoglio 等[71] 开发了含有大景深采集光学装置的在线 LIBS 系统，该系统使用固定焦点光学装置，在大范围的采样距离内保持了良好的采集效率。Moench 等[72] 首次利用在线 LIBS 装置实现了塑料瓶分拣，样品识别速率为每秒 3 个，准确率超过 87%。Stepputat 等[73] 研制了在线 LIBS 装置，实现了报废电子设备外壳中重金属元素和溴化阻燃剂的快速检测，系统自动聚焦装置的调节范围为 50 mm。
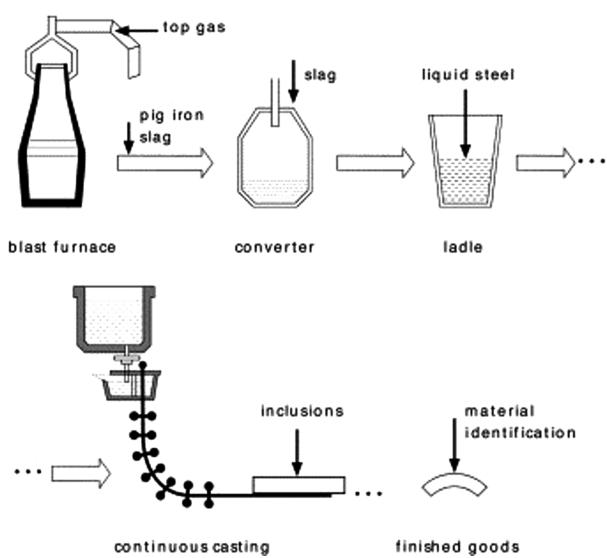
图 5　LIBS 在钢铁生产链上的应用[69]

Fig. 5　Application of LIBS in steel production chain[69]

2.2.4　便携式 LIBS 装置

便携式 LIBS 装置具有体积小、重量轻、使用方便等优点，在工业现场和野外恶劣条件下具有更好的适用性。

美国洛斯阿拉莫斯国家实验室成功研制出了世界上第一台便携式 LIBS 系统，并将其用于土壤及颜料中的金属污染物含量检测[74]。通过采用小型高分辨率光谱仪，Harmon 等[75]大大提升了便携式 LIBS 设备的现场适用性，拓宽了元素分析范围。为了方便分析艺术品及古玩等，Goujon 等[76]研制了新型、紧凑、多功能的集成便携式 LIBS设备。沙平

生等[77]设计了一套基于超小微晶片型激光器的便携式 LIBS 系统，并利用该系统实现了对多种合金样品的材料识别。王寅等[78]通过对便携式 LIBS 光学系统进行改进，成功实现了对土壤重金属的探测。方丽等[79]将半球形等离子体约束装置和多芯光纤多通道技术用于便携式 LIBS 系统，提高了光谱强度及检测灵敏度。Wormhoudt 等[80]使用一个基于微片激光器和微型光谱仪的手持式 LIBS 装置，检测了钢样品中 C 元素的含量，当 C 与 Fe 的质量分数比在 0.001～0.01 范围内时分析精密度为4.3%，检测极限为 400 mg/kg。如图 6 所示，Pérez-Diez 等[81]通过便携式 LIBS 仪器在庞贝壁画上进行检测，对光谱数据进行主成分分析，建立了卤素（CaF 和 CaCl）和相关碱金属（Na 和 K）的定性分布图，提供了有关火山卤化物的迁移和分布以及其来源（海洋气溶胶和现代固结砂浆）的信息。Rao 等[82]通过便携式 LIBS 设备对钚合金中的微量元素进行了定量分析，并使用化学计量分析来提高手持设备的灵敏度和精度，基于偏最小二乘（PLS）法确定了钚金属中 Fe 和 Ni 的检测极限分别为15 mg/kg 和 20 mg/kg。Yan 等[83]采用自主研发的手持式 LIBS 设备对岩样进行分类，利用最小标准偏差（MSD）、最小距离（MD）和威布尔分布（WD）对分布数据进行预处理，利用线性判别分析（LDA）法进行分类，分类精度分别达到 99.05%、97.04% 和 99.00%，显示了其在地质样品分析中的应用潜力。
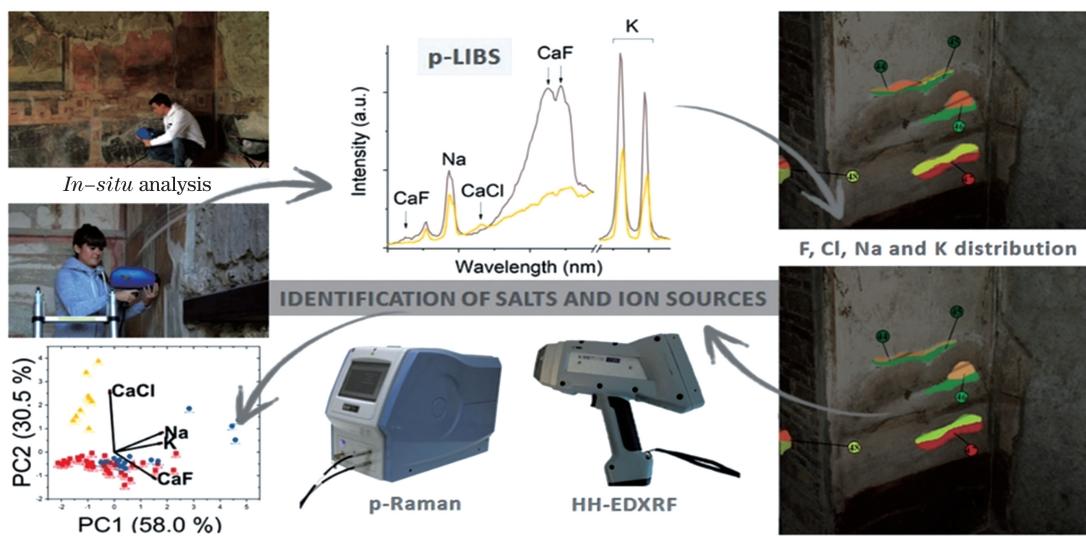

图 6　使用便携式 LIBS 装置分析庞贝壁画[81]

Fig. 6　Analysis of mural paintings of Pompeii by portable LIBS[81]

3　信号增强方法

3.1　表面增强

　　表面增强法[84-86]通过同时烧蚀衬底和待测样品,利用衬底产生的高温等离子体对样品等离子体进行加热,提高样品等离子体的温度和电子数密度。

　　衬底表面增强方法能有效克服液体检测中的液面波动、溅射和等离子体淬灭等问题,提高元素的检测极限。Alamelu 等[87]采用滤纸吸附法,实现了对水中稀土元素 Sm、Eu 和 Gd 的定量分析。Wal 等[88]研究发现,衬底种类对水中痕量元素的检测至关重要,所用衬底包括 Mg、Al、Si、Fe、Cu、玻璃、NaCl 和金属氧化物等。Jijón 等[89-90]分别采用钢铁和铝基板作为金属衬底,实现了对水溶液中 K 和 Mn 的定量分析。Matsumoto 等[91]研究了含有金纳米粒子的多孔硅衬底对表面增强 LIBS 信号稳定性的影响,7 个多孔硅衬底上的 Sr 信号的相对标准偏差约为 10%。如图 7 所示,Yang 等[92]通过增加固定区域内重复样品制备的次数,进一步提高了检测灵敏度,将重复样品制备次数从 1 增加到 8,Cu、Pb、Cr 和 Cd 的检测极限值从 0.072～0.36 mg/L 降至 0.027～0.05 mg/L。

　　纳米增强 LIBS(NELIBS)是在表面增强的基础上滴加贵金属的纳米粒子,增强效果较表面增强更加显著,分析精度改善明显。Bae 等[86]将液体滴于
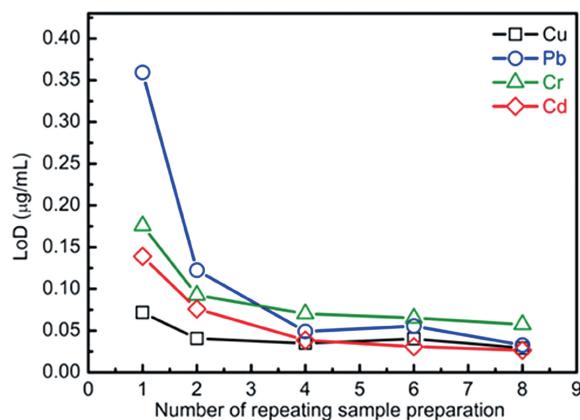
图 7　不同样品制备次数下检测极限的演变趋势[92]

Fig. 7　Evolution trend of detection limits under different numbers of sample preparations[92]

激光刻蚀过的硅片表面,发现液体扩散更为均匀,实现了单滴液体的重复性检测。如图 8 所示,de Giacomo 等[93]将含有 Pb 的溶液滴于涂有纳米金的玻璃片上,其检测极限可达 0.002 mg/L。Abdelhamid 等[94]研究了 Ag(AgCl)纳米颗粒形状(纳米球、纳米立方体和纳米线)对不同目标材料的 LIBS 信号的影响,结果表明,在 Ag 纳米线和纳米立方体中形成的簇在激光脉冲的吸收机制中起重要作用,从而增强了 LIBS 信号。Tang 等[95]研究了 NELIBS 在分子光谱领域的有效性,研究结果表明,使用较高的激光能量和较大的激光光斑直径以及对固体样品进行预烧蚀可以获得更好的增强效果。
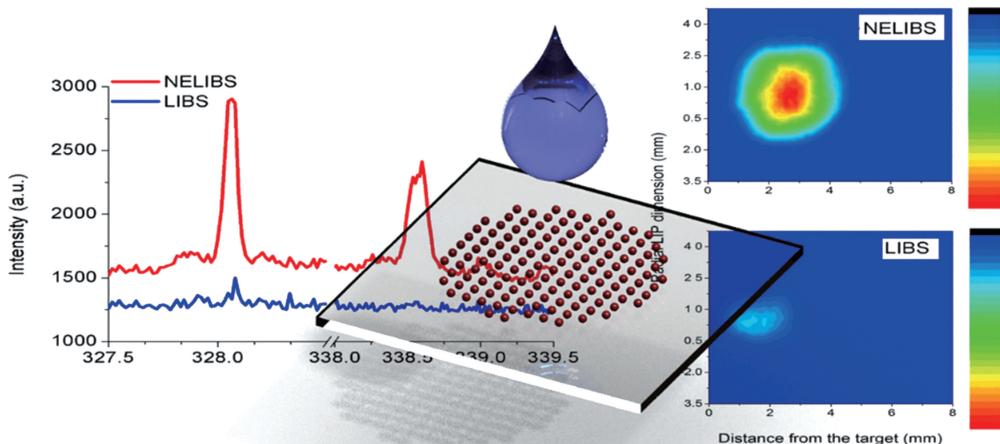

图 8　利用 NELIBS 检测溶液中的重金属元素[93]

Fig. 8　Analysis of heavy metals in solution by NELIBS[93]

3.2　惰性气体保护增强

　　惰性气体化学活性较低,利用惰性气体作为环境气体可以延长等离子体中发光原子的寿命,并能避免光信号被空气吸收[96-97]。

　　Sdorra 等[98]对比了不同气体氛围(氖气、氩气、氦气、氮气和空气)对 Cu 材料表面等离子体的影响,结果表明,在氩气氛围下,等离子体的温度更高、电子数密度更大、发射强度更高。Aragón 等[99]使用一台红外 Nd:YAG 激光器在氩气环境中分析钢铁,对于含量(质量分数)高于 0.1% 的 C、Si、Cr 和

Ni 等元素，其分析线和内标线强度比值的相对标准偏差为 0.9%～2.5%，决定系数 R^2 高于 0.9990。Sturm 等[100] 使用氩气保护的光路，对 C、P、S、Al、Cr、Cu、Mn 和 Mo 等元素进行了分析，检测极限低于 10 mg/kg，决定系数 R^2 大于 0.9900。Rajavelu 等[101] 研究了环境气体（如氦气、氮气、氩气和大气）和气体流速对开放空间中煤的 LIBS 表征的影响，

观察到 C 原子和分子（C_2 和 CN）的发射强度在氩气和氮气环境中更高。如图 9 所示，Yu 等[102] 研究了一系列由氦气、氖气和氩气组成的气体混合物对 LIBS 的各种特性（信号强度、相对标准偏差、等离子体温度）的影响，发现在由 40%（体积分数）氦气、40%（体积分数）氖气和 20%（体积分数）氩气混合而成的气体中进行 LIBS 实验可以获得最佳的综合性能。
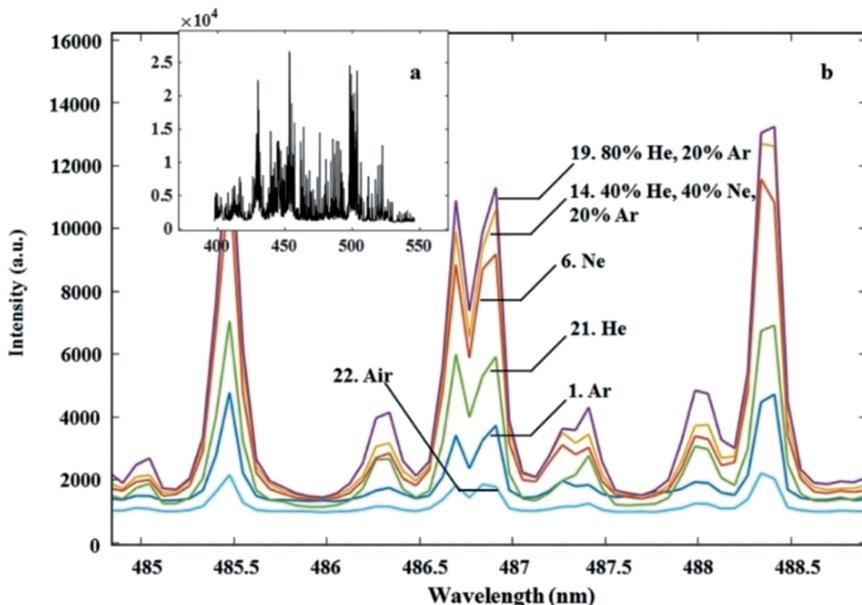

图 9　不同气体环境中钛合金样品的光谱[102]

Fig. 9　Spectra of titanium alloy samples in different gas ambient environments[102]

3.3　约束增强

约束增强利用约束腔或磁场影响等离子体的外部和内部条件，对等离子体进行约束，从而实现光谱增强。该方法简单、经济，具有很高的可行性。

激光等离子体在产生和扩散时，其外层会产生扩散速度大于等离子体扩散速度的冲击波。若冲击波在扩散的过程中遇到阻碍，会反射回来对等离子体产生反作用[103-104]。Popov 等[105] 初步研究了圆柱形腔空间约束效应对土壤光谱精密度及分析灵敏度的影响，结果发现，采用空间约束后，As、V、Pb、Mn 和 Ba 等痕量元素的分析检测极限提高为原来的 2～5 倍。Wang 等[106-107] 研究了圆柱形腔对 LIBS 分析精密度的影响，结果表明，合适尺寸的约束腔可有效约束等离子体的膨胀，降低光谱波动，改善 LIBS 的精密度。Zhao 等[108] 研究了圆柱形约束腔对飞秒 LIBS 光谱的影响，检测土壤中的 Pb 检测极限分别达到 1.45 mg/kg 和 8.85 mg/kg。Zhang 等[109] 利用不同直径（2～6 mm）和高度（1～6 mm）的铝圆柱腔获得了 LIBS 最佳约束腔尺寸（直径为

5 mm，高度为 4 mm）。

激光诱导等离子体磁约束是利用运动的带电粒子在磁场中产生的垂直于粒子运动方向的库仑力约束等离子体的膨胀，延缓了光谱强度的衰减，在确定的时延下，相当于增强了光谱强度。Rai 等[110-111] 研究了磁场对激光诱导等离子体的约束原理及其对 LIBS 的增强效应，但没有进一步研究磁约束对 LIBS 分析精密度、灵敏度和准确度的影响规律。如图 10 所示，Guo 等[112] 将磁约束和空间约束结合，将半球形空间约束腔置于一对条形磁铁产生的磁场中，同时实现了激光诱导等离子体的空间约束和磁约束，谱线强度得到了 11～22 倍的增强。Hussain 等[113] 研究了外加磁场（0.5 T）对不同气压和延迟下的 LIBS 的影响，由于磁场的影响，在低压和更短的延迟时间下观察到 Al 原子线得到显著改善。Abbasi 等[114] 通过平行于等离子体膨胀方向的磁场（0.12 T）辅助 LIBS 增强 Pd 等离子体的光发射信号，观察到 Pd 原子线和离子线的强度增强了 3～4 倍。
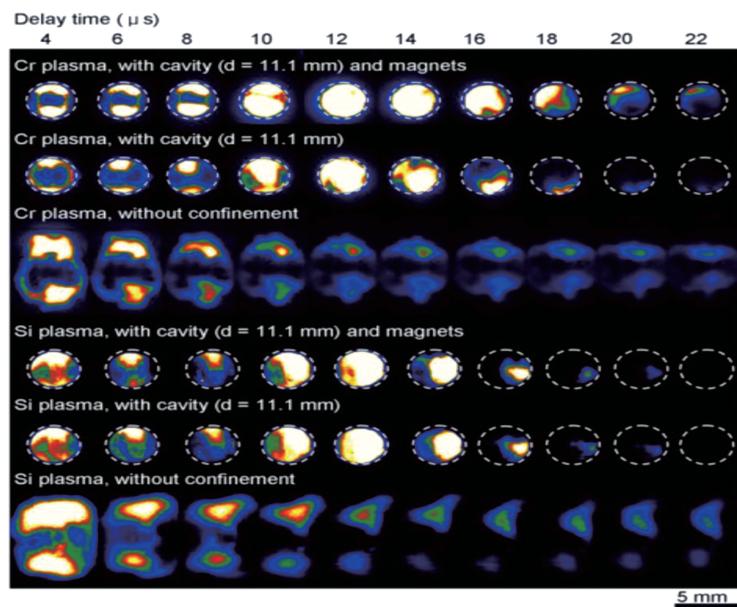
图 10   不同约束方法下 Cr 和 Si 的等离子体图像[112]

Fig. 10   Images of Cr and Si plasmas under different confinement conditions[112]

3.4 双脉冲增强

DP-LIBS 利用第二束激光脉冲对等离子体进行二次激发加热,可以大幅度提高等离子体的温度,进而增强光谱强度。

根据两束激光的入射方向和入射时序,DP-LIBS 可以分为共线型、双脉冲交叉型、再加热模式的正交型和预烧蚀模式的正交型(图 11)[115]。Colao 等[116-117]对共线 DP-LIBS 进行了研究,结果表明,高能量脉冲比低能量脉冲产生了更多更稳定的等离子体,原子或离子谱线宽度也更窄。Scaffidi 等[118]采用纳秒和飞秒脉冲激光进行正交 DP-LIBS

实验,结果表明,飞秒脉冲烧蚀的样品等离子体有较长的时间膨胀,体积较大,信号增强效果更好。Caneve 等[119]对比了单脉冲 LIBS(SP-LIBS)和 DP-LIBS 定性测量铜基合金中元素种类的效果,结果表明,双脉冲比单脉冲的烧蚀效率高、内标曲线有更好的线性趋势、热影响小以及背景辐射小。de Giacomo 等[120-121]分别利用 SP-LIBS 和 DP-LIBS 对水溶液元素和水下固体样品进行检测,证明了 DP-LIBS 技术应用于水下元素检测的可行性。林泽浩等[122]通过靶增强正交 DP-LIBS 技术进一步提高了 DP-LIBS 的增强效果,光谱强度较 DP-LIBS 增强 6 倍以上。
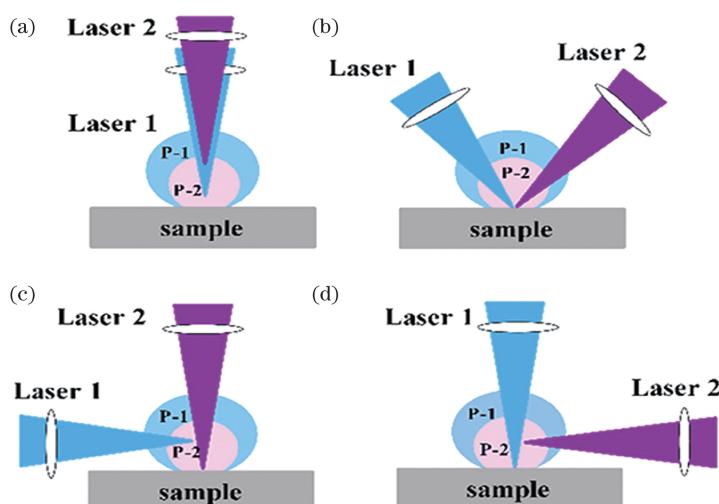
图 11   DP-LIBS 的各种配置(P-1 和 P-2 分别表示脉冲 1 和脉冲 2 产生的等离子体)[115]。(a)共线;(b)双脉冲交叉光束;(c)正交预热;(d)正交再加热

Fig. 11   Various configurations of DP-LIBS(P-1 and P-2 indicating plasmas produced by pulse 1 and pulse 2, respectively)[115]. (a) Collinear; (b) dual pulse crossed beam; (c) orthogonal preheating; (d) orthogonal reheating

共振激发（LIBS-LIF）技术是一种特殊的双脉冲技术，它首先使用激光烧蚀待测样品表面产生等离子体，再利用一束特定波长的激光辐照等离子体。该方法具有高效率和高选择性的特点，可实现指定分析元素谱线的增强，可大幅改善分析灵敏度。Hilbk-Kortenbruck 等[123]利用 LIBS-LIF 技术检测土壤中的重金属 Cd，检测极限达到 0.3 mg/kg。Li 等[124]借助 249.77 nm 激光将等离子体中处于基态的 B 原子激发至激发态，从而对其跃迁回基态的 B I 208.96 nm 荧光信号进行检测，获得镍合金中 B 的检测极限为 0.6 mg/kg。Li 等[125]利用 LIBS-LIF 技术增强了 Si I 288.16 nm 谱线强度，克服了 Fe 线干扰的问题，提高了 Si 元素的检测精度，并在一定程度上改善了自吸收效应问题。Zhou 等[126]采用 LIBS-LIF 技术有效解决了基体效应和自吸收效应对土壤微量元素定量分析的影响，检测极限均达到 mg/kg 量级。

3.5　微波增强

微波辅助增强 LIBS（MA-LIBS）是一种非常有效的 LIBS 增强方法，它通过向等离子体中注入额外的微波能量来增强 LIBS 信号。Ikeda 等[127]利用 MA-LIBS 对气体进行检测，结合微波辅助，使得 LIBS 中的 OH、N、O 和 CN 等分子及原子的谱线得到显著增强。Liu 等[128]根据等高边缘温度低的特点，使用微波对等离子体进行加热，提高了等离子体的外围温度，显著增强了 Cu 和 Ag 元素的光谱信号，分别获得了 30 mg/kg 和 23.3 mg/kg 的检测极限。Khumaeni 等[129]利用环形天线搭建 MA-LIBS 实验装置，在 1.33 kPa 大气压强和微波条件下，Gd_2O_3 样品中 Gd 谱线的增强因子达到 32，Ca 的检测极限（LoD）从 48 mg/kg 降低到 2 mg/kg。Tang 等[130]利用双针形微波辐射器来降低自吸收效应，LIBS 与 MA-LIBS 如图 12 所示，Na、K、Al、Si 和 Ca 的自吸收得到明显抑制。Wakil 等[131]探索了 MA-LIBS 利用 CaCl 分子发射检测氯的能力，Cl 的 LoD 从 170 mg/kg 降低到 47 mg/kg，检测能力提高了 3 倍。Viljanen 等[132]在大气环境下利用 MA-LIBS 实现了光谱增强，信号增强倍数达 100，Al_2O_3 样品中 Cu 的 LoD 达到 8.1 mg/kg。
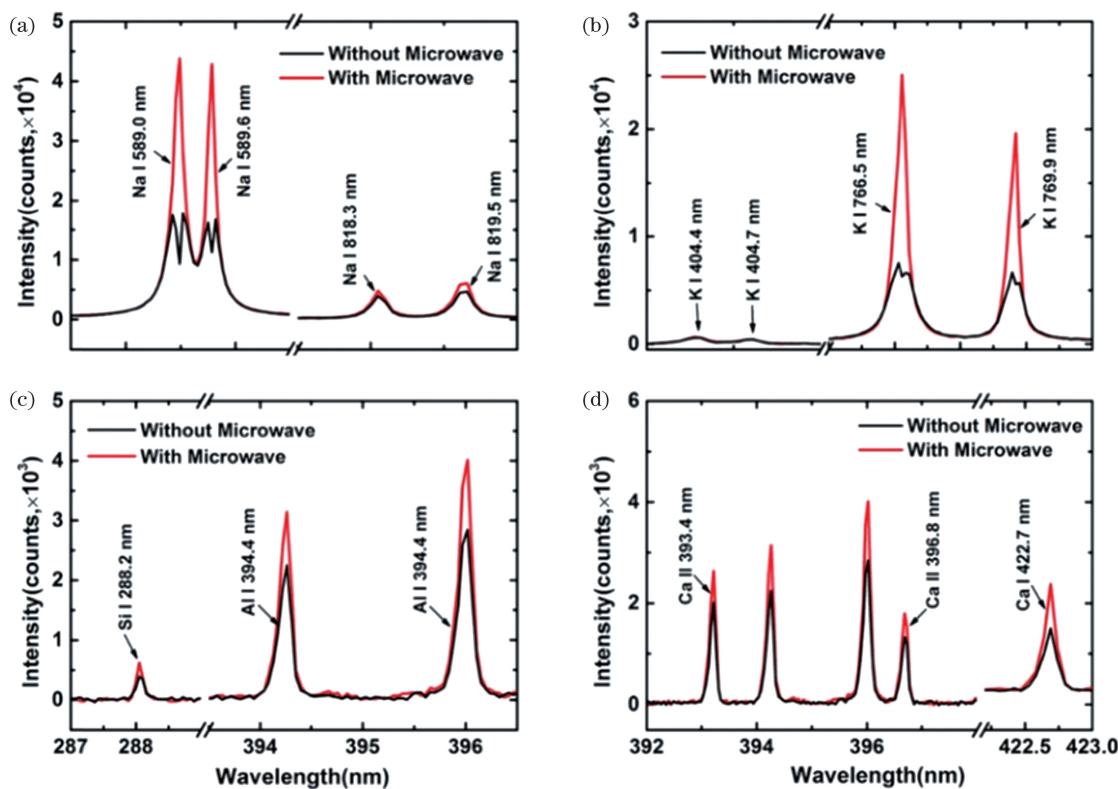

图 12　钾长石样品的 LIBS 与 MA-LIBS[130]．(a)Na；(b)K；(c)Si 和 Al；(d)Ca

Fig. 12　LIBS and MA-LIBS in potassium feldspar pellets[130]．(a) Na；(b) K；(c) Si and Al；(d) Ca

3.6　火花放电增强

火花放电增强 LIBS（SD-LIBS）是一种增强 LIBS 信号和提高检测灵敏度的低成本方法，它通过高压放电向等离子体注入能量。Zhou 等[133-136]设计了高压脉冲放电电路来辅助增强 LIBS，其电路和实验装置如图 13 所示，在检测硅片和土壤样品时，谱线的增强倍数高于 10，其中，土壤样品中 Pb、Mg 和 Sn 等微量元素的检测极限分别达到 1.5，34，0.16 mg/kg。研

究者将低功率(10 W)单极放电电弧装置和 LIBS 结合用于检测硅片,LIBS 信号得到了极大的增强,增强因子达 13.8。Ge 等[137]将激光烧蚀与常压辉光放电装置相结合来直接检测固体样品,该装置运行成本低、耗气量小,实现了对复杂基质土壤样品中 Zn、Pb、Cd 元素的高灵敏度测定,LoD 分别达到 0.68,2.71,0.31 mg/kg。
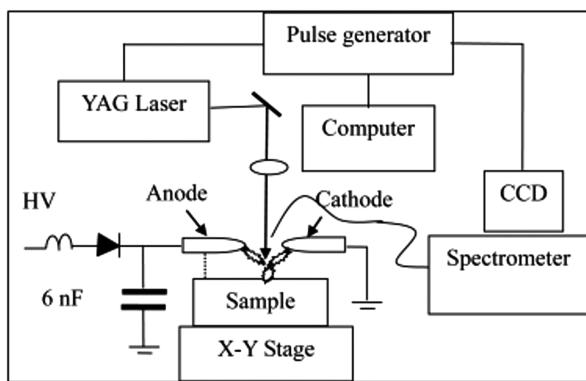

图 13　高压脉冲放电电路辅助增强 LIBS 实验装置[133-136]

Fig. 13　Experimental setup of SD-LIBS[133-136]

4　定性定量分析方法

4.1　样品分类

材料类别的准确鉴定是回收再利用的第一阶段。不同样品的 LIBS 数据存在差异,通过分析方法将这些差异提取出来就可以实现样品的分类识别。Kim 等[138]通过计算 247.9 nm 处的 C 线和 656.3 nm 处的 H 线的比率发现,不同的塑料样品的强度比值不同,分别为 0.96(聚丙烯,PP)、1.03(丙烯腈-丁二烯-苯乙烯共聚物,ABS)、1.19(聚苯乙烯,PS)和 1.42(聚对苯二甲酸乙二醇酯,PET)。Siddiqui 等[139-140]通过 C 和 H 元素的强度比实现了塑料的鉴别,高密度聚乙烯(HDPE)、低密度聚乙烯(LDPE)、PET、PP、PS 和聚氯乙烯(PVC)中 C 与 H 的强度比分别为 1.68、1.51、1.01、1.16、1.42 和 0.91,显示了 LIBS 在塑料分类领域的巨大应用潜力。Anzano 等[141]通过 C_2 516 nm、CN 388 nm、C 247.9 nm、H 656.3 nm、O 777.2 nm 和 N 746.8 nm 的强度比区分不同的塑料样品,其中,C_2 与 Cl 的强度比和 H 与 Cl 的强度比是最重要的分类指标。Barbier 等[142]发现,C_2 与 He 的强度比和 CN 与 He 的强度比有助于区分不同类别的塑料。

通过常规的分析方法即可实现大部分样品的分类识别。例如,Anzano 等[143]通过线性/等级相关方法成功识别了 5 种塑料废弃物,分类精度为 90%~

99%。此外,Anzano 等[144]将欧氏距离、欧氏距离平方、皮尔逊相关系数、曼哈顿距离方法成功应用于区分 5 种不同的塑料样品,欧氏距离是最有效的分类方法。Lasheras 等[145]利用线性/秩相关和归一化坐标(MNC)法区分 11 种塑料样品,线性/秩相关方法的分类效果更好,达到 87.3% 的识别准确率。Guo 等[146]通过 K 均值聚类(K-means)算法实现了 20 种塑料样品的聚类分析,分类精度达到 99.6%。Costa 等[147]利用偏最小二乘回归(PLSR)方法区分不同质量比的 PC/ABS 混合物,识别误差小于 10%。Costa 等[148]还利用 K 最邻近(KNN)法和簇类独立软模式(SIMCA)区分了 477 种塑料废弃物,KNN 法具有更高的分析精度,达到 98%。Ferrero 等[149]通过 MNC 方法区分了 5 种塑料样品,证明了其在区分混合物方面的独特优势。Brunnbauer[150]通过 PCA 和 K-means 方法区分了 5 种聚合物,并对其空间分布进行了分析。Yu 等[151]将 LIBS 技术与支持向量机(SVM)分类算法相结合,通过增加特定特征谱线的强度,将所有 11 种聚合物的识别准确率均提高到近 100%。孙倩倩等[152]将 LIBS 技术与 SVM 相结合,采用非金属元素特征谱线对 20 种工业塑料进行分类,识别精度达到 99.6%。

不同算法对不同样品具有不同的分析效果,将不同的算法进行整合可以摆脱单一算法的限制,显著提高模型的分类性能。Bilge 等[153]将 LIBS 技术与 PCA 和 PLS 法结合对掺杂甜乳清粉、酸乳清粉的奶粉进行分析,识别率为 80.5%,甜乳清粉和酸乳清粉的检测极限分别为 1.55% 和 0.55%。Kanawade 等[154]采集了 4 种组织 24 个样本的 LIBS,通过 PCA 方法对光谱数据进行降维分析,再结合线性判别分析(LDA)方法,实现了组织 LIBS 的分类识别,其分类准确率在 90% 以上,实验结果验证了 LIBS 作为反馈信号实现外科手术实时监测的可行性。Chen 等[155]进行了淋巴瘤患者全血和健康对照全血的 LIBS 检测。全血来自 16 个淋巴瘤患者和 17 个健康对照,采用 LDA 和 KNN 作为识别模型,其准确率高于 95%。文大鹏等[156]结合主成分分析-粒子群优化-支持向量机(PCA-PSO-SVM)算法对 12 类矿石进行分类识别,分类模型的平均识别准确率可达 99.90%。

4.2　元素识别

为了满足不同的应用需求,材料中经常添加一些辅助剂用以改善其力学和化学性能。但这些添加剂中经常含有一些有毒元素,会对人的身体健康和

生态环境造成影响。因此,对材料内的元素进行检测,能够提高材料的安全性和回收质量。

Sun 等[157]利用 LIBS 技术定性分析了人体皮肤上角质层中的微量元素,实验结果表明,LIBS 检测到的 Zn 元素浓度随着角质层的深度增加呈指数下降趋势。Stepputat 等[73]利用在线 LIBS 装置分析了报废电子电气设备中的重金属 Br、Cd、Hg、Pb、Cr 和 Sb,其检出限均低于 100 mg/kg。Lazic 等[158]利用 LIBS 技术检测了塑料样品中的 Sb 元素,检出限为 100 mg/kg 左右。Rehan 等[159]将 LIBS 用于测定印棟美容皂和印棟叶中的 Cr、Ni 和 Zn,结果表明,Ni、Cr 和 Zn 含量(质量分数)分别为 5.0～12 mg/kg、9.0～16 mg/kg 和 6.2～14 mg/kg,高于这些元素的安全允许水平。章琳颖 等[160]运用 LIBS 对赣南脐橙橙汁进行了快速绿色鉴别,分别测定了健康和黄龙病脐橙果汁的糖度及元素 Ca、K、Zn 的含量。Liu 等[161]使用 LIBS 技术检测了化妆品中的 Pb 和 Cd,检测极限分别为 0.028 mg/kg 和 0.016 mg/kg,与 ICP-MS 的结果相比,Pb 和 Cd 的相对误差分别为 3.5% 和 4.8%。Godoi 等[162]利用偏最小二乘判别分析(PLS-DA)、SIMCA 和 KNN 方法研究 51 种玩具中的有毒元素是否超标,Cd 元素的识别准确度为 95%,Cr 和 Pb 元素的识别准确度为 100%。

4.3　定量分析

类似于其他分类方法,LIBS 技术的最终目标是实现待测样品内元素的精确测定,即定量分析。但由于基体效应和自吸收效应的影响,利用 LIBS 技术进行塑料样品内元素的定量分析时,分类精度较低。

LIBS 领域最常用的定标方法为标准曲线法,它是一种传统的单变量回归方法。Sun 等[163]用 LIBS 分析铁矿石粉压片,绘制了 Mn 和 Si 元素的定标曲线,其决定系数 R^2 可达 0.99。王琦等[164]利用内标法建立钢中的 Mn 和 Cr 元素的校准曲线,检测极限分别为 50 mg/kg 和 406 mg/kg。王振南等[165]采用多条谱线峰值强度之和对钢铁中的 Mo 元素进行分析,分析值与标定值的相对误差为 7.58%。张勇等[166]采用 LIBS 技术对两块中低合金钢板坯及均匀钢样品的元素分布进行了定量分析,通过建立校准曲线,将光谱强度二维分布转化为含量二维分布,分析的空间分辨率约为 100 μm。

自由定标(CF-LIBS)方法无需标准样品,通过对 LIBS 的理论计算即可获得待分析元素的浓度。

Corsi 等[167]使用自由定标法计算人发中主要元素 Ca、Mg、K、Na 和 Al 的浓度,将计算结果与 ICP-MS 进行对比,验证了 CF-LIBS 在人发定量分析中的可行性。涂彩等[168]对黄金标准样品(Au 的质量分数为 85.0%～99.6%)进行了 LIBS 测试,采用 CF-LIBS 计算了 Au、Cu 和 Ag 三种元素的含量,结果显示,这三种元素的质量分数与标准值的误差均小于 3%。陈兴龙等[169]利用脉冲激光在空气中烧蚀炉渣样品,测定了 Ca、Mg、Al 和 Si 等元素的含量,使用 CF-LIBS 进行定量计算,结果显示,测量相对误差在 15% 之内。Roldán 等[170]使用 ns-LIBS 和 ps-LIBS 表征钨基材料,结果表明,在大气作用下,30 ps 激光下钨基材料的 CF-LIBS 定量分析结果比在 ns 激光下更精确。Miškovičová 等[171]采用 CF-LIBS 分析 Mo 合金,实现了钼合金组件的材料迁移监测和杂质检测。Hu 等[172]用柱状密度和标准参考线结合 CF-LIBS 对铝青铜和铝合金样品的元素组成进行定量分析,有效抑制了自吸收效应,并提高了 CF-LIBS 的分析精度。

多元分析方法利用已获得的数据建立分析模型,将未知样品数据输入模型即可获得分析结果,相对于标准曲线法和自由定标方法具有更高的分析精度。Death 等[173-174]采用 LIBS 结合主成分回归(PCR)法对铁矿石中的 Fe、Al、Si 和 K 进行了分析,其分析结果与 XRF 的检测结果相当,展示了 LIBS 与 PCR 相结合在铁矿石原位在线分析方面潜在的应用前景。Yaroshchyk 等[175]将 PLS 法用于铁矿石品位的检测,并与 PCR 法的结果进行了比较,结果表明,两种方法的分析精度相当,但 PLS 法使用的主成分数更少。Yaroshchyk 等[176]还将 LIBS 和 PLS 法相结合,用于对铁矿石烧失重进行定量分析,样品质量分数的均方根误差可达到 1.0%。孙兰香等[177]对钢中的 Mn 和 Si 元素进行分析时,使用人工神经网络(ANN)建立定量分析模型,与内标法相比,ANN 降低了基体效应及谱线的相互干扰,对化学体系复杂的多基体钢的分析效果更好。Moncayo 等[178]利用 LIBS 对掺杂三聚氰胺的奶粉进行鉴别,识别率达到 98%;同时采用 ANN 对 CN 分子谱线进行定量分析,标准曲线的 R^2 由 0.9820 提升到 0.9996。

5　应用研究

5.1　深空探测

人类进行深空探测的终极目标是寻找适于生命

生存的环境,对星体的物质环境进行测定成为当前的研究重点。

人类已完成了数十次与火星有关的探索任务,旨在研究火星地质演化的历史和评估人类移民火星的可能性。2011 年登陆火星的"好奇号"火星车配备的远程 LIBS 仪器——ChemCam(图 14),用于探测火星表面物质成分等信息[179-182]。美国国家航空航天局(NASA)于 2020 年发射的"毅力号"火星车除搭载了在上一代表现出色的 LIBS 仪之外,还新加入了包括 Raman 光谱仪在内的多种探测手段,结构简单的 LIBS 装置易于与其他设备联用,进一步丰富了火星车的探测能力[183]。2021 年登陆火星的中国"祝融号"火星探测器搭载的自主研发的火星表面成分探测仪(MarSCoDe),也是基于 LIBS 原理的火星物质分析仪器,用以分析火星表面和不同深度剖面上土壤矿物的化学元素组成[184-186]。
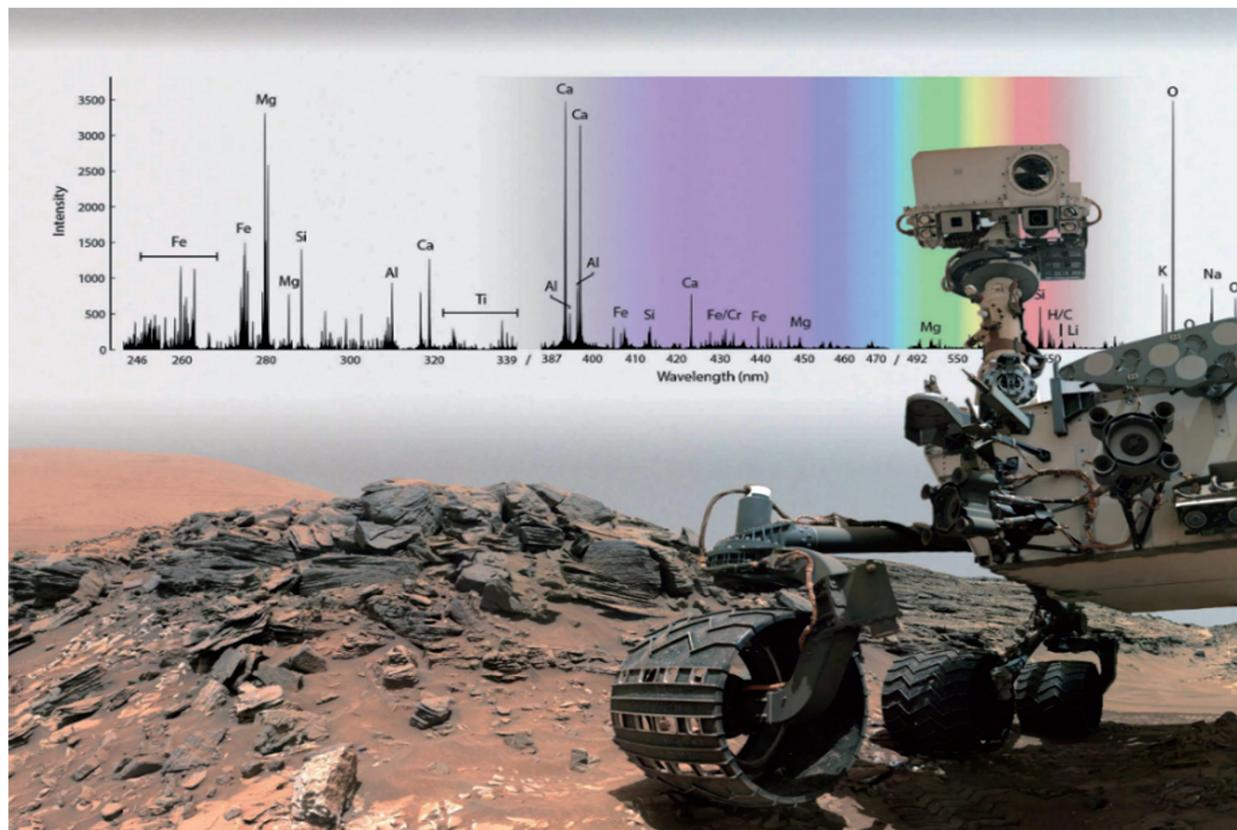
图 14 "好奇号"火星探测器对火星表面岩石的探测示意图[182]

Fig. 14　Detection schematic of rocks on surface of Mars by Curiosity rover[182]

5.2　地质勘探

地质勘探可为地层评价、矿物起源测定、矿物分布、农林及土木工程等提供关键依据。岩石成分复杂,通常包含几十种元素,传统的探测手段大多基于实验室,需要复杂和耗时的程序,时效性差。LIBS 分析迅速、可同时在线检测多种元素,对轻元素 H、Li、Be 和 B 等特别敏感,能够实现对矿物和岩石表面的亚毫米空间分辨率分析,基本不需要对样品进行预处理,同时可以应用于恶劣的自然环境甚至人类暂时无法亲临的环境,实现现场实时勘测,特别适合地质探测[187-188]。

目前,LIBS 在地质探测方面的应用多为元素识别和岩性分析。Kiros 等[189]用 LIBS 技术分析不同气候环境下岩石的元素信息。Quarles 等[190]用

LIBS 结合化学计量学方法反演岩石中氟元素的含量。Rifai 等[191]使用 LIBS 技术测定岩石样品中 Au 的浓度,富硅样品和富铁样品中 Au 的检测限分别达到 0.8 mg/kg 和 1.5 mg/kg。杨志强等[192-193]开展了一系列基于 LIBS 对地质录井岩性进行识别的相关研究,Tian 等[194-195]利用实验室 LIBS 设备进行了岩屑、火成岩和标准土壤样品识别方法的研究。Li 等[196]采用 LIBS-LIF 技术分析了矿石中的 U 元素,在提高 U 的光谱强度的同时消除了光谱干扰,LoD 达到 35 mg/kg。邱苏玲等[197]基于激光诱导击穿光谱,对铁矿石、锰矿石和铬矿石中的 Fe 元素进行了定量分析,通过相关性变量筛选偏最小二乘回归分析改进算法进行分析,发现三类矿石的预测集的均方根误差分别降至 0.975%、0.418% 和

0.123%,平均相对误差分别降至 1.46%、6.72%和 1.09%。

LIBS 的另一个独特之处是其可在高空间分辨率下对地质样品进行快速多元素组成制图。Fabre 等[198]采用 LIBS 分析热液矿石样品,绘制了面积为 5 cm² 的矿石样本表面微量元素的分布图。Kuhn 等[199]利用 LIBS 和能量色散 X 射线荧光(EDXRF)对废弃矿山的岩芯进行了面扫描分析,通过分析不同深度的岩芯表面的元素,如图 15 所示,实现了对矿产资源的勘查。Gaft 等[200]将 LIBS 和激光诱导荧光(LIF)结合,使用单一实验室设备监测样品特定位置处的激光诱导等离子体,并绘制了矿物中稀土元素的元素分布图。Sweetapple 等[201]绘制了 Li 伟晶岩矿物的分布图。El Haddad 等[202]对斑岩铜矿床的岩砖进行了矿物成像和定量分析,证明了 LIBS 在混合矿物识别和定量分析方面的能力。
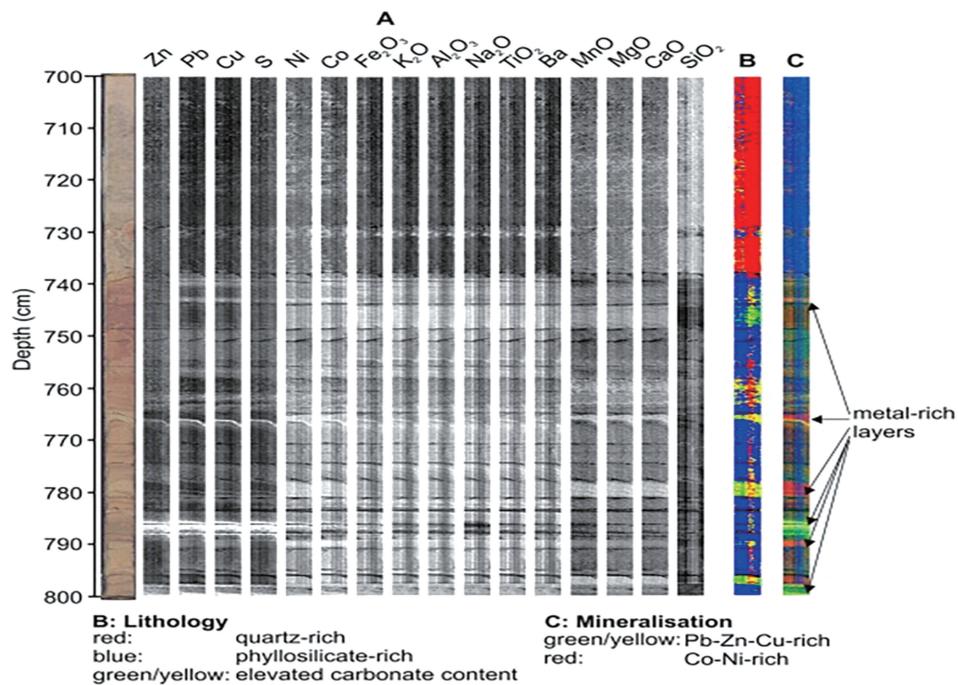
图 15 采用 LIBS 岩心扫描仪测量的岩心元素空间分布图[199]

Fig. 15 Element maps of drilled core measured with LIBS core scanner[199]

5.3 环境污染

随着工业技术的高速发展,环境污染问题也越来越严重,环境污染的实时监测对保护生态系统和人体健康具有重要意义。

当大气中的污染物累积到一定程度时,会直接和间接地对人和生物造成危害。Yan 等[203]通过 LIBS 技术对空气中的污染物进行了快速检测。研究者将 LIBS 和核极限学习机(K-ELM)组合以研究 26 个煤样中 S 的定量分析精度。Li 等[204]利用 LIBS 技术研究了不同气氛(O_2/N_2,O_2/CO_2)下煤燃烧和 NO_x 生成的机理,结果表明,生成 NO_2 需要较多的氧化气氛,其还原则需要比 NO 更多的还原气氛。空气中的硅尘在煤矿中很常见,可导致矽肺,危害极大。Stipe 等[205]开发了一种便携式监测 LIBS 装置,用于快速分析硅尘。大气中的汞具有毒性、持久性和生物累积效应。Rong 等[206]将 LIBS 用于混合气体中 Hg 的测量,结果表明,适当降低气体压力可以获得高质量的光谱信号。余英亮等[207]采用 CF-LIBS 方法对大气中的元素进行检测,实验结果与实际结果一致,证明了 LIBS 技术可应用于空气污染检测。

土壤是植物生长的必要条件,土壤污染的检测对人的身体健康和经济发展具有重要意义。Capitelli 等[208]使用 LIBS 技术检测了土壤中的 Cr、Cu 和 Pb 元素,检测极限分别为 30,30,50 mg/kg。Santos 等[209]检测了土壤中的 Cd 元素,分别采用 Cd 的特征谱线 214.4,226.5,228.8 nm 定标,在 214.44 nm 下获得了最佳 1.3 mg/kg 的检测极限。Srungaram 等[210]使用了 LIBS 技术检测土壤中的 Hg 元素,检测极限为 483 mg/kg。许洪光等[211]利用 LIBS 技术对土壤中的 Pb 元素进行定量分析,最佳检测极限达 36.7 mg/kg。王建伟等[212]总结了 LIBS 在土壤污染检测领域中的应用,并将国标检测极限与 LIBS 检测极限进行了对比。刘林美等[213]

利用 LIBS 技术定性分析了武汉地区土壤中的元素 Zn、Cu 和 Hg。鲁翠萍等[214]对土壤中的 Cr 元素进行了定量检测,检测极限达 16.5 mg/kg。潘爱民等[215]在氩气保护的条件下对土壤中的 Cd 元素进行了定量分析,检测极限达到 59 mg/kg。陈添兵等[216]分析了土壤中的元素 Ba 和 Sr,分别获得了相关系数为 0.9900 和 0.9906 的定标曲线。如图 16 所示,Yi 等[217]利用固-液-固转化样品前处理方法,通过超声振动和离心操作提取了土壤中的有效重金属,并将其沉积在玻璃片上,成功地测定了土壤中的有效态元素 Cd 和 Pb,检测极限分别达 0.067 mg/kg 和 0.940 mg/kg。Gao 等[218]对土壤中的有害元素锑(Sb)也进行了检测,检测极限达到 0.221 mg/kg。
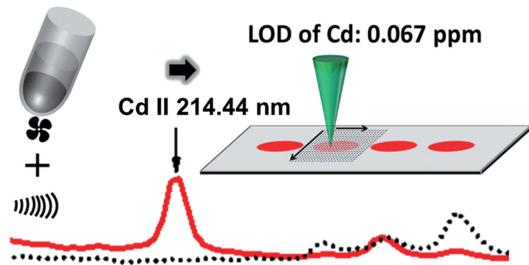
图 16 LIBS 结合固-液-固转换方法检测土壤中的有效态 Cd[217]

Fig. 16 Available Cd in soil detected by LIBS combined with solid-liquid-solid conversion method[217]

水体中的重金属元素含量超标会严重危害生物的生存环境,水体污染的高灵敏度检测对水体污染治理具有重要意义。Rai 等[219-220]将应用于标准水溶液检测的液柱法逐步推向工业废水检测,对电镀厂工业废水中的 Cr 元素的检测极限可达到 0.03 mg/L,验证了 LIBS 用于工业废水检测的可行性。Koch 等[221]利用双脉冲技术对水体中的 Mn 元素进行分析,检测极限可达 0.080 mg/L。Matsumoto 等[222]提出了一种水下电化学沉积方法,可实现水体中 Zn 元素的检测,将电沉积技术与水下 LIBS 技术结合,最终实现了质量浓度为 5 mg/L 的 Zn 元素的测量。Cheung 等[223]直接将带孔容器倒置使液体流出,然后利用 LIBS 技术对溶液中的 Na、K 和 Ba 元素进行分析,其检出限分别可达 0.23,1.5,130 mg/L。Feng 等[224]利用液体射流装置对水中重金属 Pb 进行检测,检出限为 60 mg/L。Huang 等[225]利用电喷雾电离针来产生均匀液滴,液滴在针尖下方约 2 mm 处与激光发生相互作用,最终实现了 Na、K 和 Al 元素的检测。Zhang 等[226]利用毛细管辅助方法对水中 Na 和 Cr 元素进行分析,定标曲线的决定

系数可达 0.998 以上。Yang 等[227]采用化学置换法结合表面增强 LIBS(SENLIBS)对水溶液中的痕量 Cr 元素进行检测,检出限达到 0.018 mg/L。

5.4 食品安全

农产品的质量安全问题日趋严重,加强农产品的质量检测对保障人体健康甚至生命安全至关重要。Gondal 等[228]对茶叶中的 Fe、Cr、K、Br、Cu、Si 和 Ca 元素进行了分析。Cho 等[229]利用 LIBS 技术检测面粉中的微量元素,Sr 和 Pb 的检测极限分别为 0.3 mg/kg 和 18 mg/kg。何秀文等[230]使用 SP-LIBS 技术对 Cd 污染的大米进行检测,采用单变量回归模型建立了 Cd 元素浓度与光谱强度的关系模型,检测极限为 48.14 mg/kg。Peng 等[231]将 LIBS 技术结合 PLS 对水稻叶片中的 Cr 元素进行检测,检测极限为 4.3856 mg/kg。Liu 等[232]检测了水稻中的 Cu 元素,对比了单变量和多变量回归模型进行定量分析的效果,获得的最佳检测极限为 5 mg/kg。杨晖等[233]使用 DP-LIBS 检测大米中的 Cd,检测极限为 5.06 mg/kg。胡慧琴等[234]利用微波辅助 LIBS 检测大米中的 Cd,检测极限为 2.16 mg/kg。Kim 等[235]采用 PLS-DA 辅助 LIBS 技术对菠菜是否有农药残留进行鉴别,识别率为 98%。饶刚福等[236]基于 PCA 与随机森林(RF)的结合对食品发酵产生的 10 种微生物真菌进行检测,平均识别率为 96.7%。Prochazka 等[237]采用 LIBS 技术结合自组织映射对食品中的 6 种微生物细菌菌株进行鉴别,识别率达到 100%。

肉类营养丰富,但肉类掺杂问题及饲养过程中使用违禁药物问题会严重危害人的身体健康。Bilge 等[238]采用 LIBS 技术结合 PCA 算法对猪肉、牛肉、鸡肉粉末样品掺杂进行鉴别,平均识别率为 83.37%。Yueh 等[239]使用 PCA、PLS-DA、层次聚类分析(HCA)和反向传播人工神经网络(BP-ANN)四种分类模型分别对冻鸡肉不同部位组织进行 LIBS 检测,最佳平均识别率为 93.18%。朱毅宁等[240]运用 PCA 结合 SVM 模型对新鲜的猪肉、牛肉和鸡肉组织进行直接检测,平均识别率为 89.11%。陈添兵等[241]利用不同的光谱预处理方法对组织样本的 LIBS 光谱进行预处理,以探究其对定量分析结果的影响;采用 PLSR 实现了猪肉中 Pb 的定量分析;为了提高光谱的稳定性,采用多元散射校正(MSC)作为光谱预处理方法,最终采用 MSC-PLS 混合模型实现了元素的定量分析,模型预测值和元素检测值的决定系数高达 0.99。

食用油是人体重要的营养以及能量来源，也是食品加工制造产业的重要基础原料。为保障广大人民群众的身体健康，食用油的快速、高效检测方法的研究迫在眉睫。吴鼎等[242]基于 PCA 与 ANN 对地沟油、豆油、调和油进行鉴别，地沟油的识别率为 94.2%。朱泉水等[243]利用 PCA 和 PLS 成功实现了对掺假浓度的预测，预测误差小于 2%。Caceres 等[244]采用 LIBS 技术对西班牙市面上的橄榄油掺假情况进行调查，平均识别率达到 95%。Gazeli 等[245]将 LIBS 与机器学习算法相结合，根据酸度和产地对橄榄油进行分类，分类准确度达到 90.0%～99.2%。如图 17 所示，Bellou 等[246]研究了不同

LIBS 实验装置（喷雾、层流、液面）对橄榄油分类的影响，通过将 LIBS 与机器学习方法 PCA 和 LDA 等相结合，获得了有关橄榄油样品产地和掺假的信息，分类准确率达到 100%。Gyftokostas 等[247]根据地理来源对特级初榨橄榄油和原生橄榄油样本进行区分，结果表明，机器学习辅助 LIBS 在橄榄油鉴别中有巨大的应用潜力。Stefas 等[248]利用 LIBS 和吸收光谱辅助机器学习技术，对不同品种的希腊特级初榨橄榄油进行鉴别，使用 LDA 和梯度提升算法进行分类，结果表明，在机器学习算法的帮助下，这种方法在橄榄油认证和分类方面具有很高的应用潜力。
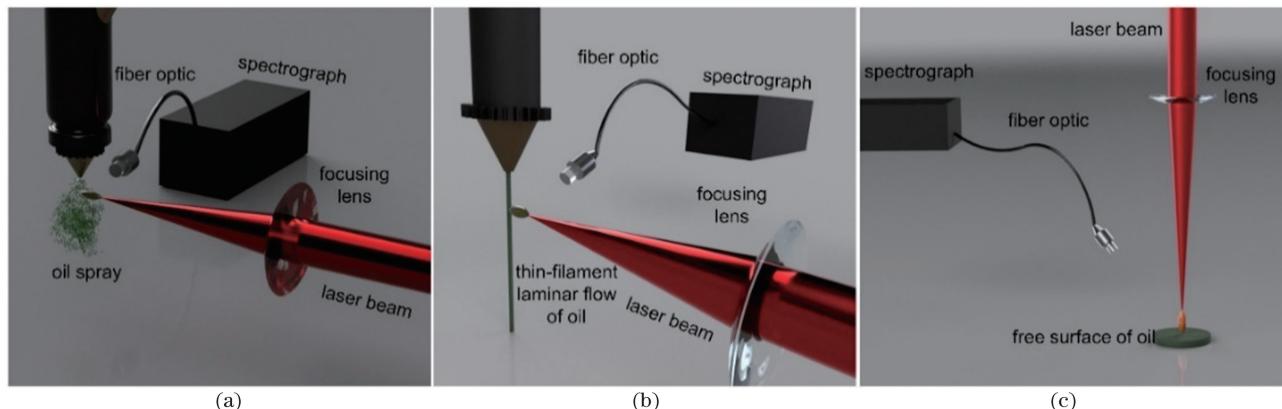
图 17   LIBS 实验中橄榄油的处理方法[246]。(a)喷雾法；(b)层流法；(c)静置油样法

Fig. 17   Methods for handling olive oil samples in LIBS experiments[246]. (a) Spray method; (b) laminar flow method; (c) method of resting oil samples

5.5   工业冶金

航空航天等技术的发展和人们生活水平的不断提高对金属性能也有了更高的要求。快速获取金属材料的成分信息成为当前的研究热点之一。

钢铁是应用最为广泛的金属材料，实现钢铁内元素的快速、高灵敏度检测对改善钢铁性能具有重要意义。Vrenegor 等[249]为了解决高合金钢中微量和痕量元素检测的基体效应，引入了一种多重迭代校正的方法。Bredice 等[38]为了研究锰铁合金中 Mn 元素谱线的自吸收问题，利用谱线强度比计算自吸收系数。Sun 等[39]采用内参考线校正自吸收，成功实现了铬铁合金的 CF-LIBS 检测。Mermet 等[250]提出一种归一化方法来改善激光脉冲能量波动对光谱分析精密度的影响。Peter 等[96]在真空紫外环境下，采用三脉冲激发 LIBS 方法对钢液中的多种元素进行了定量分析，元素 C、P、S、Ni 和 Cr 的检测极限分别为 5，21，11，9 ，9 mg/kg。2014 年，Sturm 等[251]采用 LIBS 技术对某钢厂的液渣进行在线分析，如图 18 所示，实现了钢包不同充填水平

的自动测量，测量时间仅为 2 min，在连续 3 个月的试用期间，实现了 7 d（每天 24 h）的稳定运行。

实现高性能合金的快速检测可以为相关行业现有难题的解决提供技术支持。Tsai 等[252]采用 3.0 mJ 的 Nd∶YAG 激光在20 Pa 氩气环境中激发镍基合金等离子体，镍基合金中 Al、Si 的检测极限分别为 53 mg/kg 和 92 mg/kg，分析误差小于 10%。Zhu 等[253]采用 LIBS 技术分析镍基高温合金中的 Al 元素，检测极限为 0.09%～0.1%。Gupta 等[254]采用 355 nm 激光在空气中分析镍基合金中质量分数为 16.67%～25.01%的 Cr 元素，取得了良好的定量分析效果。Kim 等[255]采用 LIBS 技术分析了镍基合金表面氧化层中 Mn、Cr、Ni、Al 和 Ti 等元素沿厚度方向的分布，其结果与 XRF、扫描电镜-能谱仪（SEM-EDS）和二次离子质谱（SIMS）等传统手段的检测结果吻合良好，显示了 LIBS 技术在研究高温合金氧化机制方面的巨大应用潜力。Shen 等[256]采用 LIBS-LIF 分析钛合金中的钇（Y）元素，其检出限为 0.3 mg/kg，R^2 达到 0.9950。

(a)　　　　　　　　　　　　　(b)　　　　　　　　　　　　　(c)
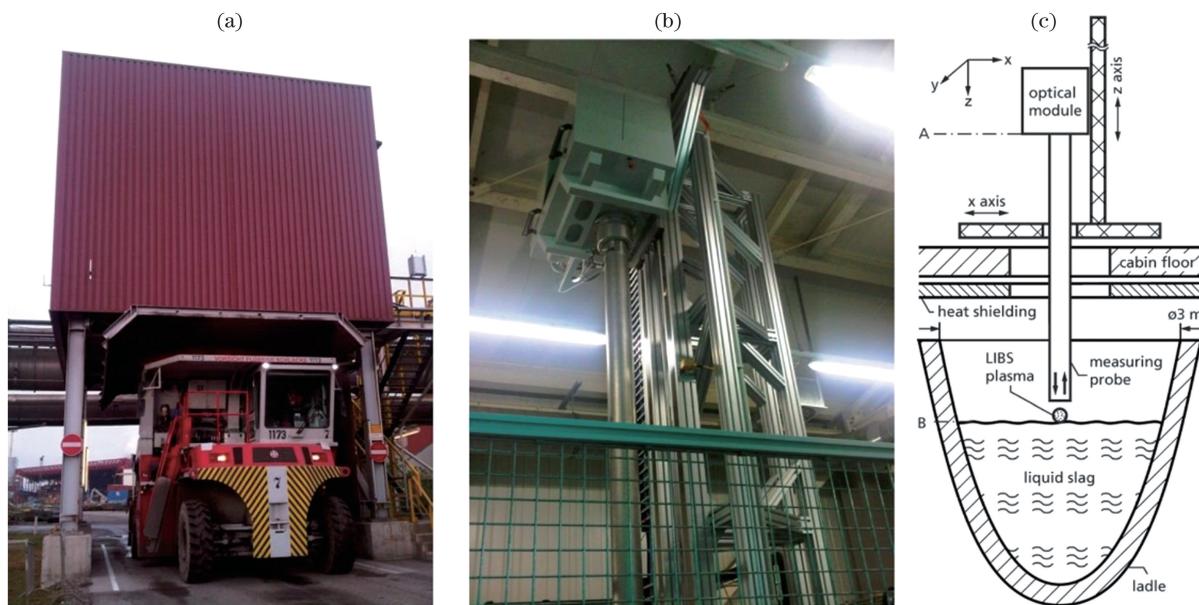
图 18　LIBS 液渣在线分析[251]。(a)分析时在测量舱下装有钢包的运渣机；(b)通过安装在电动 x 轴和 z 轴上的光模块和测量探头观察测量座舱内部；(c)LIBS 分析仪安装示意图

Fig. 18　On-line analysis of liquid slag by LIBS[251]. (a) Slag transporter with ladle during analysis underneath measuring cabin; (b) view inside measuring cabin with optical module and measuring probe mounted at motorized x- and z-axes; (c) schematic of installing LIBS analyzer

5.6　生物医疗

传统的病理活检方法存在样品制备过程复杂、耗时长的问题，开发一种更新、更快、更有效的生物医疗辅助技术具有重要意义。图 19 展示了 LIBS 成像分析在 3D 分析、代谢动力学等中的应用[257]。
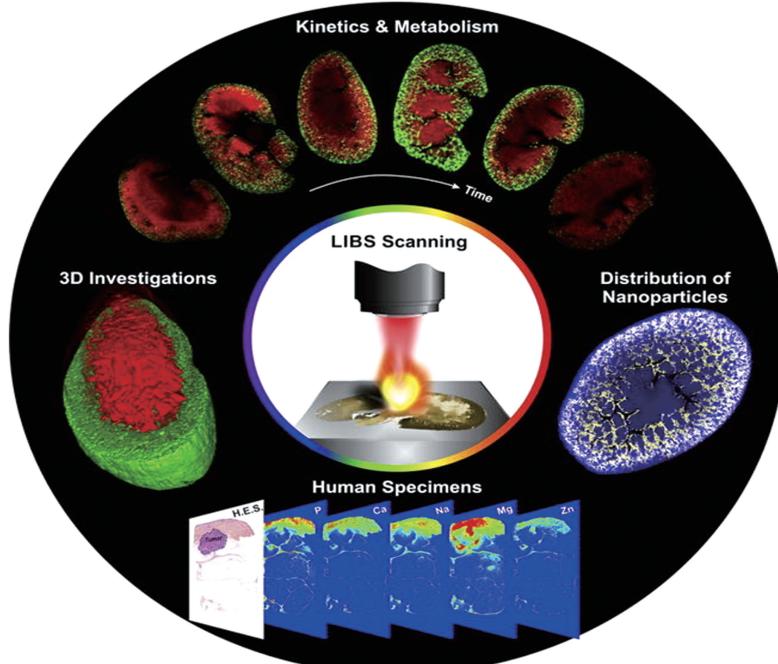
图 19　生物组织的 LIBS 扫描分析[257]

Fig. 19　Scanning and analysis of biological tissues using LIBS[257]

实现肿瘤的快速筛查能够缩短治疗周期和减少成本。Kumar 等[258]实现了最早的 LIBS 肿瘤组织识别。采用狗肝作为实验对象，采集正常狗肝组织和血管肉瘤的 LIBS，结果表明，不同的元素谱线强度比值可以用来进行肿瘤和正常组织的分类，例如 Ca 元素和 Al 元素在正常组织中的光谱强度高于肿

瘤组织的,同时采用电感耦合等离子体发射光谱对 LIBS 的检测结果进行了验证。Han 等[259]利用 LIBS 分析了黑色素瘤,并着重对比了组织中的 Ca 元素和 Mg 元素。实验中将黑色素瘤植入到小老鼠体内,然后采集癌组织和正常组织的 LIBS。实验结果表明,Ca 和 Mg 可以作为肿瘤组织和正常组织的生物标记。针对光谱识别,采用 PCA 结合 LDA 实现了两种类型的组织区分,其分类的敏感度和特异性均高于 95%。Chen 等[260]研究了淋巴瘤、多发性骨髓瘤和健康对照血清的 LIBS 差异,利用 KNN 对光谱进行分类识别,针对二分类问题,采用接受者操作特性(ROC)的曲线下面积(AUC)作为分类识别结果的评价指标,其中针对淋巴瘤、多发性骨髓瘤的 AUC 均大于 0.95。Markushin 等[261]采用飞秒 LIBS(fs-LIBS)检测了卵巢癌生物标志物 CA125,实验结果表明,光谱的变异系数低于 3%。基于 fs-LIBS 的标志物检测,其最低的检测结果低于酶联免疫吸附测定方法,同时也低于其他商业检测手段。

钙化组织和血细胞在一定程度上也可以反映生物体的饮食和健康情况。Samek 等[262]使用 LIBS 检测了钙化组织中的主要元素和潜在的有毒元素,制作了牙齿、骨骼中 Al、Pb、Sr 元素的一维及两维分布图。Bilmes 等[263]采用 LIBS 对牙齿中的 Ca 和 Sr 进行检测,实现了不同时期的饮食习惯分析。Hamzaoui 等[264]发现,在正常人和灰指甲患者指甲的 LIBS 中,Ca、Na 和 K 的光谱强度分布存在显著差异,并利用谱峰强度比获取了 Ca 与 K、Na 与 K 的相对浓度。Ng 等[265]采用 193 nm 激光烧蚀鞘流中的血细胞,捕获并分析了单个消融细胞的等离子体发射光谱,测出 Na 和 K 的光谱强度与连续介质背景的均方根波动的比值分别为 18 和 30。

6　总结与展望

简要介绍了 LIBS 技术的研究进展,包括 LIBS 技术的机理、LIBS 装置的类型、信号增强方法、定性定量分析方法以及应用领域。LIBS 技术以其独特的优势,在深空探测、地质勘探、环境污染、食品安全、工业冶金和生物医疗等领域发展成为一种强有力的快检技术。

样品类别的快速鉴定是目前的研究重点之一,且取得了不错的结果。然而,由于实验环境的变化、样品表面脏污以及制作工艺和添加剂的多样性等问题,LIBS 技术对真实样品的预测精度较低。异常值筛选、变量选择、尺度变换等光谱预处理方法以及算

法的改进和整合将是解决这一问题的有效途径。由于基体效应、激光能量波动、光谱仪分辨率差异、检测环境限制等原因,LIBS 技术对材料内元素含量的预测偏差较大。优化 LIBS 仪器平台、研究信号增强方法和改进分析方法将是提高定量分析预测准确度的有效方法。

基体效应是限制 LIBS 技术广泛应用的最为关键的问题。随着 LIBS 仪器及相应组件的不断研发,该问题能够得到有效解决,但这将需要很长时间。而分析化学方法的改进将是提高 LIBS 技术应用性能的有效途径。为了实现海量材料的快速、高灵敏度检测,在线 LIBS 装置的研制将是未来的发展趋势。

参 考 文 献

[1] 龙海珍, 王景凤, 王茂盛, 等. 火试金富集—重量法测定锌阳极泥中银含量的方法[J]. 有色金属科学与工程, 2019, 10(6): 76-80.
Long H Z, Wang J F, Wang M S, et al. Determination of silver content in zinc anode slime by fire assay gravimetry method[J]. Nonferrous Metals Science and Engineering, 2019, 10(6): 76-80.

[2] 沈文馨, 章效强, 杨戈, 等. EDTA 容量法测定氧化镧中稀土总量的不确定度评定[J]. 中国检验检测, 2017, 25(3): 37-40.
Shen W X, Zhang X Q, Yang G, et al. Evaluation of the uncertainty for determination of total rare earth in Lanthanum oxide by EDTA volumetric method[J]. China Inspection Body & Laboratory, 2017, 25(3): 37-40.

[3] 张静, 程琳, 林琳, 等. 基于谷胱甘肽识别系统的胶体金比色法快速检测水中重金属铅离子[J]. 食品科学, 2017, 38(24): 202-207.
Zhang J, Cheng L, Lin L, et al. Gold nanoparticles-based glutathione recognition for rapid colorimetric detection of lead ion in water[J]. Food Science, 2017, 38(24): 202-207.

[4] Olesik J W. Elemental analysis using ICP-OES and ICP/MS[J]. Analytical Chemistry, 1991, 63(1): 12A-21A.

[5] Ammann A A. Inductively coupled plasma mass spectrometry (ICP MS): a versatile tool[J]. Journal of Mass Spectrometry, 2007, 42(4): 419-427.

[6] Smith E, Dent G. Modern Raman spectroscopy—a practical approach[M]. Chichester: John Wiley & Sons, Ltd., 2004.

[7] Jones R R, Hooper D C, Zhang L W, et al. Raman techniques: fundamentals and frontiers[J]. Nanoscale Research Letters, 2019, 14(1): 231.

［8］ Workman J, Jr, Shenk J. Understanding and using the near-infrared spectrum as an analytical method ［J］. Near-infrared Spectroscopy in Agriculture, 2004, 44: 1-10.

［9］ Bokobza L. Near infrared spectroscopy［J］. Journal of Near Infrared Spectroscopy, 1998, 6(1): 3-17.

［10］ Hou X D, He Y H, Jones B T. Recent advances in portable X-ray fluorescence spectrometry［J］. Applied Spectroscopy Reviews, 2004, 39(1): 1-25.

［11］ Potts P J, Webb P C. X-ray fluorescence spectrometry ［J］. Journal of Geochemical Exploration, 1992, 44 (1/2/3): 251-296.

［12］ García R, Báez A P. Atomic absorption spectrometry (AAS) ［M］// Farrukh M A. Atomic absorption spectroscopy. London: InTech, 2012.

［13］ Ferreira S L C, Bezerra M A, Santos A S, et al. Atomic absorption spectrometry—a multi element technique［J］. TrAC Trends in Analytical Chemistry, 2018, 100: 1-6.

［14］ Miziolek A W, Palleschi V, Schechter I. Laser-induced breakdown spectroscopy (LIBS): fundamentals and applications［J］. Critical Reviews in Analytical Chemistry, 2006, 27(4): 257-290.

［15］ Cremers D A, Radziemski L J. Handbook of laser-induced breakdown spectroscopy ［M］. Chichester, UK: John Wiley & Sons, Ltd., 2006.

［16］ Singh J P, Almirall J R, Sabsabi M, et al. Laser-induced breakdown spectroscopy (LIBS) ［J］. Analytical and Bioanalytical Chemistry, 2011, 400 (10): 3191-3192.

［17］ Hahn D W, Omenetto N. Laser-induced breakdown spectroscopy (LIBS), part I: review of basic diagnostics and plasma-particle interactions: still-challenging issues within the analytical plasma community［J］. Applied Spectroscopy, 2010, 64 (12): 335-366.

［18］ Hahn D W, Omenetto N. Laser-induced breakdown spectroscopy (LIBS), part II: review of instrumental and methodological approaches to material analysis and applications to different fields ［J］. Applied Spectroscopy, 2012, 66(4): 347-419.

［19］ Fortes F J, Moros J, Lucena P, et al. Laser-induced breakdown spectroscopy［J］. Analytical Chemistry, 2013, 85(2): 640-669.

［20］ Li W T, Li X Y, Li X, et al. A review of remote laser-induced breakdown spectroscopy［J］. Applied Spectroscopy Reviews, 2020, 55(1): 1-25.

［21］ Guo K M, Chen A M, Xu W P, et al. Effect of sample temperature on time-resolved laser-induced breakdown spectroscopy［J］. AIP Advances, 2019, 9 (6): 065214.

［22］ Hansen P B, Schröder S, Kubitza S, et al. Modeling of time-resolved LIBS spectra obtained in Martian atmospheric conditions with a stationary plasma approach［J］. Spectrochimica Acta Part B: Atomic Spectroscopy, 2021, 178: 106115.

［23］ Kumar P, Soumyashree S, Rao Epuru N, et al. Determination of stark shifts and widths using time resolved laser-induced breakdown spectroscopy (LIBS) measurements ［J］. Applied Spectroscopy, 2020, 74(8): 913-920.

［24］ Hemalaxmi R, Vasa N J, Seshadri S. Understanding the mechanism of molecular carbon emissions using time-resolved LIBS during online coal characterization ［C］// 14th Pacific Rim Conference on Lasers and Electro-Optics (CLEO PR 2020), August 3-5, 2020, Sydney, Australia. Washington, D.C.: OSA, 2020: P3_19.

［25］ Wang Q Y, Chen A M, Xu W P, et al. Time-resolved spectroscopy of femtosecond laser-induced Cu plasma with spark discharge［J］. Plasma Science and Technology, 2019, 21(6): 065504.

［26］ Ghezelbash M, Majd A E, Darbani S M R, et al. Spatial investigation of plasma emission from laminar diffusion methanol, ethanol, and n-propanol alcohol flames using LIBS method［J］. Applied Physics B, 2016, 123(1): 1-14.

［27］ Li X F, gao Q, Han L, et al. The spatial resolution of nanosecond laser-induced plasma spectroscopy in gases ［J］. Journal of Analytical Atomic Spectrometry, 2021, 36(5): 993-998.

［28］ Mal E, Junjuri R, Gundawar M K, et al. Spatial characterization of ns-laser induced Tungsten plasma in air using laser induced breakdown spectroscopy ［J］. Fusion Engineering and Design, 2021, 173: 112839.

［29］ Aragón C, Aguilera J A. Two-dimensional spatial distribution of the time-integrated emission from laser-produced plasmas in air at atmospheric pressure ［J］. Applied Spectroscopy, 1997, 51(11): 1632-1638.

［30］ Corsi M, Cristoforetti G, Giuffrida M, et al. Three-dimensional analysis of laser induced plasmas in single and double pulse configuration ［ J ］. Spectrochimica Acta Part B: Atomic Spectroscopy, 2004, 59(5): 723-735.

［31］ Xiu J S, Bai X S, Negre E, et al. Indirect laser-induced breakdown of transparent thin gel layer for sensitive trace element detection［J］. Applied Physics Letters, 2013, 102(24): 244101.

［32］ Bai X S, Ma Q L, Motto-Ros V, et al. Convoluted effect of laser fluence and pulse duration on the

property of a nanosecond laser-induced plasma into an argon ambient gas at the atmospheric pressure［J］. Journal of Applied Physics, 2013, 113(1): 013304.

［33］ Yu J, Ma Q L, Motto-Ros V, et al. Generation and expansion of laser-induced plasma as a spectroscopic emission source［J］. Frontiers of Physics, 2012, 7 (6): 649-669.

［34］ Amamou H, Bois A, Ferhat B, et al. Correction of self-absorption spectral line and ratios of transition probabilities for homogeneous and LTE plasma［J］. Journal of Quantitative Spectroscopy and Radiative Transfer, 2002, 75(6): 747-763.

［35］ El Sherbini A M, El Sherbini T M, Hegazy H, et al. Evaluation of self-absorption coefficients of aluminum emission lines in laser-induced breakdown spectroscopy measurements［J］. Spectrochimica Acta Part B: Atomic Spectroscopy, 2005, 60(12): 1573-1579.

［36］ Aguilera J A, Aragón C. Characterization of laser-induced plasmas by emission spectroscopy with curve-of-growth measurements. Part I: temporal evolution of plasma parameters and self-absorption［J］. Spectrochimica Acta Part B: Atomic Spectroscopy, 2008, 63(7): 784-792.

［37］ Aragón C, Aguilera J A. CSigma graphs: a new approach for plasma characterization in laser-induced breakdown spectroscopy［J］. Journal of Quantitative Spectroscopy and Radiative Transfer, 2014, 149: 90-102.

［38］ Bredice F, Borges F O, Sobral H, et al. Evaluation of self-absorption of manganese emission lines in Laser Induced Breakdown Spectroscopy measurements［J］. Spectrochimica Acta Part B: Atomic Spectroscopy, 2006, 61(12): 1294-1303.

［39］ Sun L X, Yu H B. Correction of self-absorption effect in calibration-free laser-induced breakdown spectroscopy by an internal reference method［J］. Talanta, 2009, 79(2): 388-395.

［40］ Hou J J, Zhang L, Yin W B, et al. Development and performance evaluation of self-absorption-free laser-induced breakdown spectroscopy for directly capturing optically thin spectral line and realizing accurate chemical composition measurements［J］. Optics Express, 2017, 25(19): 23024-23034.

［41］ Chen J Z, Ma R L, Wang J, et al. Detection of the elements Mn and Ni in a steel sample by laser-induced breakdown spectroscopy［J］. Acta Photonica Sinica, 2014, 43(12): 1214001.

［42］ Moon H Y, Herrera K K, Omenetto N, et al. On the usefulness of a duplicating mirror to evaluate self-absorption effects in laser induced breakdown spectroscopy［J］. Spectrochimica Acta Part B:

Atomic Spectroscopy, 2009, 64(7): 702-713.

［43］ Burger M, Skočić M, Bukvić S. Study of self-absorption in laser induced breakdown spectroscopy ［J］. Spectrochimica Acta Part B: Atomic Spectroscopy, 2014, 101: 51-56.

［44］ Yi R X, Guo L B, Li C M, et al. Investigation of the self-absorption effect using spatially resolved laser-induced breakdown spectroscopy［J］. Journal of Analytical Atomic Spectrometry, 2016, 31(4): 961-967.

［45］ Li J M, Guo L B, Li C M, et al. Self-absorption reduction in laser-induced breakdown spectroscopy using laser-stimulated absorption［J］. Optics Letters, 2015, 40(22): 5224-5226.

［46］ Li J M, Tang Y, Hao Z Q, et al. Evaluation of the self-absorption reduction of minor elements in laser-induced breakdown spectroscopy assisted with laser-stimulated absorption［J］. Journal of Analytical Atomic Spectrometry, 2017, 32(11): 2189-2193.

［47］ Hao Z Q, Liu L, Shen M, et al. Investigation on self-absorption at reduced air pressure in quantitative analysis using laser-induced breakdown spectroscopy ［J］. Optics Express, 2016, 24(23): 26521-26528.

［48］ Zeng Q, Sirven J B, Gabriel J C P, et al. Laser induced breakdown spectroscopy for plastic analysis ［J］. TrAC Trends in Analytical Chemistry, 2021, 140: 116280.

［49］ Fink H, Panne U, Niessner R. Analysis of recycled thermoplasts from consumer electronics by laser-induced plasma spectroscopy［J］. Analytica Chimica Acta, 2001, 440(1): 17-25.

［50］ Wang Q Q, Jander P, Fricke-Begemann C, et al. Comparison of 1064 nm and 266 nm excitation of laser-induced plasmas for several types of plastics and one explosive［J］. Spectrochimica Acta Part B: Atomic Spectroscopy, 2008, 63(10): 1011-1015.

［51］ Negre E, Motto-Ros V, Pelascini F, et al. Classification of plastic materials by imaging laser-induced ablation plumes［J］. Spectrochimica Acta Part B: Atomic Spectroscopy, 2016, 122: 132-141.

［52］ Viskup R, Praher B, Linsmeyer T, et al. Influence of pulse-to-pulse delay for 532 nm double-pulse laser-induced breakdown spectroscopy of technical polymers［J］. Spectrochimica Acta Part B: Atomic Spectroscopy, 2010, 65(11): 935-942.

［53］ Moros J, Lorenzo J A, Lucena P, et al. Simultaneous Raman spectroscopy-laser-induced breakdown spectroscopy for instant standoff analysis of explosives using a mobile integrated sensor platform［J］. Analytical Chemistry, 2010, 82(4): 1389-1400.

[54] Hoehse M, Mory D, Florek S, et al. A combined laser-induced breakdown and Raman spectroscopy Echelle system for elemental and molecular microanalysis [J]. Spectrochimica Acta Part B: Atomic Spectroscopy, 2009, 64(11/12): 1219-1227.

[55] Shameem K M M, Choudhari K S, Bankapur A, et al. A hybrid LIBS-Raman system combined with chemometrics: an efficient tool for plastic identification and sorting [J]. Analytical and Bioanalytical Chemistry, 2017, 409(13): 3299-3308.

[56] Liu Y, Bousquet B, Baudelet M, et al. Improvement of the sensitivity for the measurement of copper concentrations in soil by microwave-assisted laser-induced breakdown spectroscopy[J]. Spectrochimica Acta Part B: Atomic Spectroscopy, 2012, 73: 89-92.

[57] Jiang T J, Guo Z, Ma M J, et al. Electrochemical laser induced breakdown spectroscopy for enhanced detection of Cd(II) without interference in rice on layer-by-layer assembly of graphene oxides [J]. Electrochimica Acta, 2016, 216: 188-195.

[58] Liu P, Wu D, Sun L Y, et al. Laser-induced breakdown spectroscopy to monitor ion cyclotron range of frequency wall cleaning Li/D co-deposition in EAST tokamak[J]. Fusion Engineering and Design, 2017, 118: 98-103.

[59] Xiao Q, Hai R, Ding H, et al. *In-situ* analysis of the first wall by laser-induced breakdown spectroscopy in the TEXTOR tokamak: dependence on the magnetic field strength[J]. Journal of Nuclear Materials, 2015, 463: 911-914.

[60] Sun L X, Xin Y, Cong Z B, et al. Online compositional analysis of molten steel by laser-induced breakdown spectroscopy [J]. Advanced Materials Research, 2013, 694/695/696/697: 1260-1266.

[61] Guirado S, Fortes F J, Laserna J J. Elemental analysis of materials in an underwater archeological shipwreck using a novel remote laser-induced breakdown spectroscopy system[J]. Talanta, 2015, 137: 182-188.

[62] Fortes F J, Guirado S, Metzinger A, et al. A study of underwater stand-off laser-induced breakdown spectroscopy for chemical analysis of objects in the deep ocean [J]. Journal of Analytical Atomic Spectrometry, 2015, 30(5): 1050-1056.

[63] Li W T, Yang X Y, Li X, et al. A portable multi-collector system based on an artificial optical compound eye for stand-off laser-induced breakdown spectroscopy [J]. Journal of Analytical Atomic Spectrometry, 2017, 32(10): 1975-1979.

[64] Homma T, Kumada A, Fujii T, et al. Depth profiling of surface degradation of silicone rubber composite insulators by remote laser-induced breakdown spectroscopy [J]. Spectrochimica Acta Part B: Atomic Spectroscopy, 2021, 180: 106206.

[65] Kokkinaki O, Klini A, Polychronaki M, et al. Assessing the type and quality of high voltage composite outdoor insulators by remote laser-induced breakdown spectroscopy analysis: a feasibility study [J]. Spectrochimica Acta Part B: Atomic Spectroscopy, 2020, 165: 105768.

[66] Junjuri R, Gummadi A P, Gundawar M K. Single-shot compact spectrometer based standoff LIBS configuration for explosive detection using artificial neural networks[J]. Optik, 2020, 204: 163946.

[67] Gaft M, Sapir-Sofer I, Modiano H, et al. Laser induced breakdown spectroscopy for bulk minerals online analyses [J]. Spectrochimica Acta Part B: Atomic Spectroscopy, 2007, 62(12): 1496-1503.

[68] Noll R, Fricke-Begemann C, Brunk M, et al. Laser-induced breakdown spectroscopy expands into industrial applications[J]. Spectrochimica Acta Part B: Atomic Spectroscopy, 2014, 93: 41-51.

[69] Noll R, Bette H, Brysch A, et al. Laser-induced breakdown spectrometry: applications for production control and quality assurance in the steel industry[J]. Spectrochimica Acta Part B: Atomic Spectroscopy, 2001, 56(6): 637-649.

[70] Zhang L, Ma W G, Dong L, et al. Development of an apparatus for on-line analysis of unburned carbon in fly ash using laser-induced breakdown spectroscopy (LIBS) [J]. Applied Spectroscopy, 2011, 65(7): 790-796.

[71] Redoglio D A, Golinelli E, Musazzi S, et al. Development of a large depth of field collection optics for on-line laser-induced breakdown spectroscopy applications[J]. Spectrochimica Acta Part B: Atomic Spectroscopy, 2016, 123: 179-183.

[72] Moench I, Sattmann R, Noll R. High-speed identification of polymers by laser-induced breakdown spectroscopy[J]. Proceedings of SPIE, 1997, 3100: 1-11.

[73] Stepputat M, Noll R. On-line detection of heavy metals and brominated flame retardants in technical polymers with laser-induced breakdown spectrometry [J]. Applied Optics, 2003, 42(30): 6210-6220.

[74] Yamamoto K Y, Cremers D A, Ferris M J, et al. Detection of metals in the environment using a portable laser-induced breakdown spectroscopy instrument[J]. Applied Spectroscopy, 1996, 50(2): 222-233.

[75] Harmon R S, de Lucia F C, Munson C A, et al.

Laser-induced breakdown spectroscopy（LIBS）: an emerging field-portable sensor technology for real-time chemical analysis for military, security and environmental applications[J]. Proceedings of SPIE, 2005, 5994: 59940K.

[76] Goujon J, Giakoumaki A, Piñon V, et al. A compact and portable laser-induced breakdown spectroscopy instrument for single and double pulse applications [J]. Spectrochimica Acta Part B: Atomic Spectroscopy, 2008, 63(10): 1091-1096.

[77] 沙平生, 禹素萍, 聂朝江, 等. 基于超小微晶片激光的便携式 LIBS 系统的实现[J]. 仪表技术, 2011(1): 13-15, 18.
Sha P S, Yu S P, Nie C J, et al. Portable laser-induced breakdown spectroscopy system based on ultra-small microchip laser [J]. Instrumentation Technology, 2011(1): 13-15, 18.

[78] 王寅, 赵南京, 马明俊, 等. 便携式土壤重金属探测仪光学结构设计[J]. 光学技术, 2012, 38(5): 551-554.
Wang Y, Zhao N J, Ma M J, et al. Optical structure design of portable soil heavy metal detector [J]. Optical Technique, 2012, 38(5): 551-554.

[79] 方丽, 赵南京, 马明俊, 等. 激光诱导击穿光谱结合标准加入法定量分析土壤中铅、镉、铬和铜[J]. 光谱学与光谱分析, 2017(10): 3274-3280.
Fang L, Zhao N J, Ma M J, et al. Quantitative analysis of Pb, Cd, Cr and Cu in soil using standard addition method combined with laser-induced breakdown spectroscopy [J]. Spectroscopy and Spectral Analysis, 2017(10): 3274-3280.

[80] Wormhoudt J, Iannarilli F J, Jr, Jones S, et al. Determination of carbon in steel by laser-induced breakdown spectroscopy using a microchip laser and miniature spectrometer [J]. Applied Spectroscopy, 2005, 59(9): 1098-1102.

[81] Pérez-Diez S, Fernández-Menéndez L J, Veneranda M, et al. Chemometrics and elemental mapping by portable LIBS to identify the impact of volcanogenic and non-volcanogenic degradation sources on the mural paintings of Pompeii[J]. Analytica Chimica Acta, 2021, 1168: 338565.

[82] Rao A P, Jenkins P R, Vu D M, et al. Rapid quantitative analysis of trace elements in plutonium alloys using a handheld laser-induced breakdown spectroscopy （LIBS） device coupled with chemometrics and machine learning[J]. Analytical Methods: Advancing Methods and Applications, 2021, 13(30): 3368-3378.

[83] Yan J J, Yang P, Zhou R, et al. Classification accuracy improvement by data preprocessing in handheld laser-induced breakdown spectroscopy[J]. Analytical Methods, 2019, 11(40): 5177-5184.

[84] Yang X Y, Hao Z Q, shen M, et al. Simultaneous determination of La, Ce, Pr, and Nd elements in aqueous solution using surface-enhanced laser-induced breakdown spectroscopy [J]. Talanta, 2017, 163: 127-131.

[85] Tian Y, Cheung H C, Zheng R E, et al. Elemental analysis of powders with surface-assisted thin film laser-induced breakdown spectroscopy [J]. Spectrochimica Acta Part B: Atomic Spectroscopy, 2016, 124: 16-24.

[86] Bae D S, Nam S H, Han S H, et al. Spreading a water droplet on the laser-patterned silicon wafer substrate for surface-enhanced laser-induced breakdown spectroscopy [J]. Spectrochimica Acta Part B: Atomic Spectroscopy, 2015, 113: 70-78.

[87] Alamelu D, Sarkar A, Aggarwal S K. Laser-induced breakdown spectroscopy for simultaneous determination of Sm, Eu and Gd in aqueous solution [J]. Talanta, 2008, 77(1): 256-261.

[88] Wal R L V, Ticich T M, West J R, Jr, et al. Trace metal detection by laser-induced breakdown spectroscopy[J]. Applied Spectroscopy, 1999, 53 (10): 1226-1236.

[89] Jijón D, Costa C. Pencil lead scratches on steel surfaces as a substrate for LIBS analysis of dissolved salts in liquids[J]. Journal of Physics: Conference Series, 2011, 274: 012077.

[90] Aguirre M A, Legnaioli S, Almodóvar F, et al. Elemental analysis by surface-enhanced laser-induced breakdown spectroscopy combined with liquid-liquid microextraction[J]. Spectrochimica Acta Part B: Atomic Spectroscopy, 2013, 79/80: 88-93.

[91] Matsumoto A, Shimazu Y, Nakano H, et al. Signal stability of surface-enhanced laser-induced breakdown spectroscopy for microdroplet analysis using a porous silicon substrate[J]. Spectrochimica Acta Part B: Atomic Spectroscopy, 2021, 178: 106143.

[92] Yang X Y, Li X Y, Cui Z F, et al. Improving the sensitivity of surface-enhanced laser-induced breakdown spectroscopy by repeating sample preparation[J]. Frontiers in Physics, 2020, 8: 194.

[93] de Giacomo A, Koral C, Valenza G, et al. Nanoparticle enhanced laser-induced breakdown spectroscopy for microdrop analysis at subppm level [J]. Analytical Chemistry, 2016, 88(10): 5251-5257.

[94] Abdelhamid M, Attia Y A, Abdel-Harith M. The significance of nano-shapes in nanoparticle-enhanced laser-induced breakdown spectroscopy[J]. Journal of

Analytical Atomic Spectrometry, 2020, 35（12）: 2982-2989.

[95] Tang Z Y, Liu K, Hao Z Q, et al. The validity of nanoparticle enhanced molecular laser-induced breakdown spectroscopy［J］. Journal of Analytical Atomic Spectrometry, 2021, 36(5): 1034-1040.

[96] Peter L, Sturm V, Noll R. Liquid steel analysis with laser-induced breakdown spectrometry in the vacuum ultraviolet［J］. Applied Optics, 2003, 42 (30): 6199-6204.

[97] Jiang X, Hayden P, Costello J T, et al. Double-pulse laser induced breakdown spectroscopy with ambient gas in the vacuum ultraviolet: optimization of parameters for detection of carbon and sulfur in steel［J］. Spectrochimica Acta Part B: Atomic Spectroscopy, 2014, 101: 106-11

[98] Sdorra W, Niemax K. Basic investigations for laser microanalysis: III. Application of different buffer gases for laser-produced sample plumes ［J］. Microchimica Acta, 1992, 107(3/4/5/6): 319-327.

[99] Aragón C, Aguilera J A, Peñalba F. Improvements in quantitative analysis of steel composition by laser-induced breakdown spectroscopy at atmospheric pressure using an infrared Nd∶YAG laser［J］. Applied Spectroscopy, 1999, 53(10): 1259-1267.

[100] Sturm V, Vrenegor J, Noll R, et al. Bulk analysis of steel samples with surface scale layers by enhanced laser ablation and LIBS analysis of C, P, S, Al, Cr, Cu, Mn and Mo［J］. Journal of Analytical Atomic Spectrometry, 2004, 19(4): 451-456.

[101] Rajavelu H, Vasa N J, Seshadri S. Effect of ambiance on the coal characterization using laser-induced breakdown spectroscopy（LIBS）［J］. Applied Physics A, 2020, 126(6): 1-10.

[102] Yu J L, Hou Z Y, Ma Y Y, et al. Improvement of laser induced breakdown spectroscopy signal using gas mixture［J］. Spectrochimica Acta Part B: Atomic Spectroscopy, 2020, 174: 105992.

[103] Shen X K, Sun J, Ling H, et al. Spatial confinement effects in laser-induced breakdown spectroscopy［J］. Applied Physics Letters, 2007, 91 (8): 081501.

[104] Wang Y, Yuan H, Fu Y T, et al. Experimental and computational investigation of confined laser-induced breakdown spectroscopy［J］. Spectrochimica Acta Part B: Atomic Spectroscopy, 2016, 126: 44-52.

[105] Popov A M, Colao F, Fantoni R. Spatial confinement of laser-induced plasma to enhance LIBS sensitivity for trace elements determination in soils ［J］. Journal of Analytical Atomic

Spectrometry, 2010, 25(6): 837.

[106] Wang Z, Hou Z Y, Lui S L, et al. Utilization of moderate cylindrical confinement for precision improvement of laser-induced breakdown spectroscopy signal［J］. Optics Express, 2012, 20 (S6): A1011-A1018.

[107] Su X J, Zhou W D, Qian H G. Optimization of cavity size for spatial confined laser-induced breakdown spectroscopy［J］. Optics Express, 2014, 22(23): 28437-28442.

[108] Zhao S Y, Gao X, Chen A M, et al. Effect of spatial confinement on Pb measurements in soil by femtosecond laser-induced breakdown spectroscopy ［J］. Applied Physics B, 2019, 126(1): 1-6.

[109] Zhang L L, Yang Y W. Optimally enhanced optical emission in laser-induced breakdown spectroscopy by combining a cylindrical cavity confinement and Au-Nanoparticles action ［J］. Optik, 2020, 220: 165129.

[110] Rai V N, Rai A K, Yueh F Y, et al. Optical emission from laser-induced breakdown plasma of solid and liquid samples in the presence of a magnetic field［J］. Applied Optics, 2003, 42(12): 2085-2093.

[111] Shen X K, Lu Y F, Gebre T, et al. Optical emission in magnetically confined laser-induced breakdown spectroscopy ［J］. Journal of Applied Physics, 2006, 100(5): 053303.

[112] Guo L B, Hu W, Zhang B Y, et al. Enhancement of optical emission from laser-induced plasmas by combined spatial and magnetic confinement ［J］. Optics Express, 2011, 19(15): 14067-14075.

[113] Hussain A, Asghar H, Iqbal T, et al. Improving the spectral intensity of aluminum plasma by applied-magnetic field in laser-induced breakdown spectroscopy［J］. Optik, 2022, 251: 168220.

[114] Abbasi S A, Aziz Z, Khan T M, et al. Enhancement of optical signal and characterization of palladium plasma by magnetic field-assisted laser-induced breakdown spectroscopy［J］. Optik, 2020, 224: 165746.

[115] Fu X L, Li G L, Dong D M. Improving the detection sensitivity for laser-induced breakdown spectroscopy: a review［J］. Frontiers in Physics, 2020, 8: 68.

[116] Colao F, Pershin S, Lazic V, et al. Investigation of the mechanisms involved in formation and decay of laser-produced plasmas ［J］. Applied Surface Science, 2002, 197/198: 207-212.

[117] Colao F, Lazic V, Fantoni R, et al. A comparison of single and double pulse laser-induced breakdown

spectroscopy of aluminum samples［J］. Spectrochimica Acta Part B: Atomic Spectroscopy, 2002, 57(7): 1167-1179.

[118] Scaffidi J, Pender J, Pearman W, et al. Dual-pulse laser-induced breakdown spectroscopy with combinations of femtosecond and nanosecond laser pulses［J］. Applied Optics, 2003, 42(30): 6099-6106.

[119] Caneve L, Colao F, Fantoni R, et al. Laser ablation of copper based alloys by single and double pulse laser induced breakdown spectroscopy［J］. Applied Physics A, 2006, 85(2): 151-157.

[120] de Giacomo A, Dell'Aglio M, de Pascale O, et al. From single pulse to double pulse ns-laser induced breakdown spectroscopy under water: elemental analysis of aqueous solutions and submerged solid samples［J］. Spectrochimica Acta Part B: Atomic Spectroscopy, 2007, 62(8): 721-738.

[121] de Giacomo A, Dell'Aglio M, Bruno D, et al. Experimental and theoretical comparison of single-pulse and double-pulse laser induced breakdown spectroscopy on metallic samples［J］. Spectrochimica Acta Part B: Atomic Spectroscopy, 2008, 63(7): 805-816.

[122] 林泽浩, 李润华, 姜银花, 等. 靶增强正交双脉冲激光诱导击穿光谱的信号增强机制研究［J］. 中国激光, 2021, 48(24): 2411001.
Lin Z H, Li R H, Jiang Y H, et al. Signal enhancement in target-enhanced orthogonal double-pulse laser-induced breakdown spectroscopy［J］. Chinese Journal of Lasers, 2021, 48(24): 2411001.

[123] Hilbk-Kortenbruck F, Noll R, Wintjens P, et al. Analysis of heavy metals in soils using laser-induced breakdown spectrometry combined with laser-induced fluorescence［J］. Spectrochimica Acta Part B: Atomic Spectroscopy, 2001, 56(6): 933-945.

[124] Li C M, Hao Z Q, Zou Z M, et al. Determinations of trace boron in superalloys and steels using laser-induced breakdown spectroscopy assisted with laser-induced fluorescence［J］. Optics Express, 2016, 24(8): 7850-7857.

[125] Li J M, Xu M L, Ma Q X, et al. Sensitive determination of silicon contents in low-alloy steels using micro laser-induced breakdown spectroscopy assisted with laser-induced fluorescence［J］. Talanta, 2019, 194: 697-702.

[126] Zhou R, Liu K, Tang Z Y, et al. Determination of micronutrient elements in soil using laser-induced breakdown spectroscopy assisted by laser-induced fluorescence［J］. Journal of Analytical Atomic Spectrometry, 2021, 36(3): 614-621.

[127] Ikeda Y, Moon A, Kaneko M. Development of microwave-enhanced spark-induced breakdown spectroscopy［J］. Applied Optics, 2010, 49(13): C95-C100.

[128] Liu Y, Baudelet M, Richardson M. Elemental analysis by microwave-assisted laser-induced breakdown spectroscopy: evaluation on ceramics［J］. Journal of Analytical Atomic Spectrometry, 2010, 25(8): 1316-1323.

[129] Khumaeni A, Motonobu T, Katsuaki A, et al. Enhancement of LIBS emission using antenna-coupled microwave［J］. Optics Express, 2013, 21(24): 29755-29768.

[130] Tang Y, Li J M, Hao Z Q, et al. Multielemental self-absorption reduction in laser-induced breakdown spectroscopy by using microwave-assisted excitation［J］. Optics Express, 2018, 26(9): 12121-12130.

[131] Wakil M A, Alwahabi Z T. Quantitative fluorine and bromine detection under ambient conditions via molecular emission［J］. Journal of Analytical Atomic Spectrometry, 2020, 35(11): 2620-2626.

[132] Viljanen J, Sun Z W, Alwahabi Z T. Microwave assisted laser-induced breakdown spectroscopy at ambient conditions［J］. Spectrochimica Acta Part B: Atomic Spectroscopy, 2016, 118: 29-36.

[133] Zhou W D, Li K X, Li X F, et al. Development of a nanosecond discharge-enhanced laser plasma spectroscopy［J］. Optics Letters, 2011, 36(15): 2961-3963.

[134] Zhou W D, Li K X, Shen Q M, et al. Optical emission enhancement using laser ablation combined with fast pulse discharge［J］. Optics Express, 2010, 18(3): 2573-2578.

[135] Li K X, Zhou W D, Shen Q M, et al. Laser ablation assisted spark induced breakdown spectroscopy on soil samples［J］. Journal of Analytical Atomic Spectrometry, 2010, 25(9): 1475-1481.

[136] Li X F, Zhou W D, Li K X, et al. Laser ablation fast pulse discharge plasma spectroscopy analysis of Pb, Mg and Sn in soil［J］. Optics Communications, 2012, 285(1): 54-58.

[137] Ge F, Gao L, Peng X X, et al. Atmospheric pressure glow discharge optical emission spectrometry coupled with laser ablation for direct solid quantitative determination of Zn, Pb, and Cd in soils［J］. Talanta, 2020, 218: 121119.

[138] Kim E, Choi W Z. Real-time identification of plastics by types using laser-induced breakdown spectroscopy［J］. Journal of Material Cycles and Waste Management, 2019, 21(1): 176-180.

［139］ Siddiqui M N, Gondal M A, Redhwi H H. Identification of different type of polymers in plastics waste［J］. Journal of Environmental Science and Health. Part A, Toxic/Hazardous Substances & Environmental Engineering, 2008, 43(11): 1303-1310.

［140］ Gondal M A, Siddiqui M N. Identification of different kinds of plastics using laser-induced breakdown spectroscopy for waste management［J］. Journal of Environmental Science and Health, Part A, 2007, 42(13): 1989-1997.

［141］ Anzano J, Lasheras R J, Bonilla B, et al. Classification of polymers by determining of C_1:C_2:CN:H:N:O ratios by laser-induced plasma spectroscopy (LIPS)［J］. Polymer Testing, 2008, 27(6): 705-710.

［142］ Barbier S, Perrier S, Freyermuth P, et al. Plastic identification based on molecular and elemental information from laser induced breakdown spectra: a comparison of plasma conditions in view of efficient sorting［J］. Spectrochimica Acta Part B: Atomic Spectroscopy, 2013, 88: 167-173.

［143］ Anzano J, Casanova M E, Bermúdez M S, et al. Rapid characterization of plastics using laser-induced plasma spectroscopy (LIPS)［J］. Polymer Testing, 2006, 25(5): 623-627.

［144］ Anzano J, Bonilla B, Montull-Ibor B, et al. Classifications of plastic polymers based on spectral sata analysis with leaser induced breakdown spectroscopy［J］. Journal of Polymer Engineering, 2010, 30(3/4): 177-188.

［145］ Lasheras R J, Bello-Gálvez C, Rodríguez-Celis E M, et al. Discrimination of organic solid materials by LIBS using methods of correlation and normalized coordinates［J］. Journal of Hazardous Materials, 2011, 192(2): 704-713.

［146］ Guo Y M, Tang Y, Du Y, et al. Cluster analysis of polymers using laser-induced breakdown spectroscopy with K-means［J］. Plasma Science and Technology, 2018, 20(6): 065505.

［147］ Costa V C, Aquino F W B, Paranhos C M, et al. Use of laser-induced breakdown spectroscopy for the determination of polycarbonate (PC) and acrylonitrile-butadiene-styrene (ABS) concentrations in PC/ABS plastics from e-waste［J］. Waste Management, 2017, 70: 212-221.

［148］ Costa V C, Aquino F W B, Paranhos C M, et al. Identification and classification of polymer e-waste using laser-induced breakdown spectroscopy (LIBS) and chemometric tools［J］. Polymer Testing, 2017, 59: 390-395.

［149］ Ferrero A, Lucena P, Herrera R G, et al. Libraries for spectrum identification: method of normalized coordinates versus linear correlation［J］. Spectrochimica Acta Part B: Atomic Spectroscopy, 2008, 63(3): 383-388.

［150］ Brunnbauer L, Larisegger S, Lohninger H, et al. Spatially resolved polymer classification using laser induced breakdown spectroscopy (LIBS) and multivariate statistics［J］. Talanta, 2020, 209: 120572.

［151］ Yu Y, Guo L B, Hao Z Q, et al. Accuracy improvement on polymer identification using laser-induced breakdown spectroscopy with adjusting spectral weightings［J］. Optics Express, 2014, 22(4): 3895-3901.

［152］ 孙倩倩, 杜敏, 郭连波, 等. 塑料激光诱导击穿光谱技术快速分类应用研究［J］. 光谱学与光谱分析, 2017, 37(7): 2205-2209.
Sun Q Q, Du M, Guo L B, et al. Fast identification of plastics with laser-induced breakdown spectroscopy［J］. Spectroscopy and Spectral Analysis, 2017, 37(7): 2205-2209.

［153］ Bilge G, Sezer B, Eseller K E, et al. Determination of whey adulteration in milk powder by using laser induced breakdown spectroscopy［J］. Food Chemistry, 2016, 212: 183-188.

［154］ Kanawade R, Mehari F, Knipfer C, et al. Pilot study of laser induced breakdown spectroscopy for tissue differentiation by monitoring the plume created during laser surgery: an approach on a feedback laser control mechanism［J］. Spectrochimica Acta Part B: Atomic Spectroscopy, 2013, 87: 175-181.

［155］ Chen X, Li X H, Yang S B, et al. Discrimination of lymphoma using laser-induced breakdown spectroscopy conducted on whole blood samples［J］. Biomedical Optics Express, 2018, 9(3): 1057-1068.

［156］ 文大鹏, 梁西银, 苏茂根, 等. 激光诱导击穿光谱技术结合 PCA-PSO-SVM 对矿石分类识别［J］. 激光与光电子学进展, 2021, 58(23): 2314006.
Wen D P, Liang X Y, Su M G, et al. Classification of ores using laser-induced breakdown spectroscopy combined with PCA-PSO-SVM［J］. Laser & Optoelectronics Progress, 2021, 58(23): 2314006.

［157］ Sun Q, Tran M, Smith B, et al. *In-situ* evaluation of barrier-cream performance on human skin using laser-induced breakdown spectroscopy［J］. Contact Dermatitis, 2000, 43(5): 259-263.

［158］ Lazic V, Filella M, Turner A. Determination of antimony concentrations in widely used plastic

objects by laser induced breakdown spectroscopy (LIBS)［J］. Journal of Analytical Atomic Spectrometry, 2018, 33(11): 1917-1924.

[159] Rehan I, Gondal M A, Rehan K, et al. Nondestructive determination of chromium, nickel, and zinc in neem leaves and facial care products by laser induced breakdown spectroscopy (LIBS)［J］. Analytical Letters, 2022, 55(6): 990-1003.

[160] 章琳颖, 黎静, 饶洪辉, 等. 基于 LIBS 的黄龙病脐橙元素检测与品质鉴别［J］. 激光与光电子学进展, 2020, 57(23): 233002.
Zhang L Y, Li J, Rao H H, et al. LIBS-based element detection and quality identification of huanglongbing navel oranges ［J］. Laser & Optoelectronics Progress, 2020, 57(23): 233002.

[161] Liu Y C, Chu Y W, Hu Z L, et al. High-sensitivity determination of trace lead and cadmium in cosmetics using laser-induced breakdown spectroscopy with ultrasound-assisted extraction［J］. Microchemical Journal, 2020, 158: 105322.

[162] Godoi Q, Leme F O, Trevizan L C, et al. Laser-induced breakdown spectroscopy and chemometrics for classification of toys relying on toxic elements ［J］. Spectrochimica Acta Part B: Atomic Spectroscopy, 2011, 66(2): 138-143.

[163] Sun Q, Tran M, Smith B W, et al. Determination of Mn and Si in iron ore by laser-induced plasma spectroscopy［J］. Analytica Chimica Acta, 2000, 413(1/2): 187-195.

[164] 王琦, 陈兴龙, 余嵘华, 等. 基于激光诱导击穿光谱技术对钢中 Mn 和 Cr 元素的定量分析［J］. 光谱学与光谱分析, 2011, 31(9): 2546-2551.
Wang Q, Chen X L, Yu R H, et al. Quantitative analysis of Mn, Cr in steel based on laser-induced breakdown spectroscopy ［J］. Spectroscopy and Spectral Analysis, 2011, 31(9): 2546-2551.

[165] 王振南, 李颖, 张庆玉, 等. 激光诱导击穿光谱技术定量分析钢铁合金中痕量 Mo 元素实验研究［J］. 光谱学与光谱分析, 2011, 31(6): 1697-1701.
Wang Z N, Li Y, Zhang Q Y, et al. Experimental investigation of quantitatively analysing trace Mo in complex metallic alloys by laser induced breakdown spectroscopy ［J］. Spectroscopy and Spectral Analysis, 2011, 31(6): 1697-1701.

[166] 张勇, 贾云海, 陈吉文, 等. 激光诱导击穿光谱法对钢铁偏析样品的分析［J］. 光谱学与光谱分析, 2013, 33(12): 3383-3387.
Zhang Y, Jia Y H, Chen J W, et al. Segregation bands analysis of steel sample using laser-induced breakdown spectroscopy ［J］. Spectroscopy and Spectral Analysis, 2013, 33(12): 3383-3387.

[167] Corsi M, Cristoforetti G, Hidalgo M, et al. Application of laser-induced breakdown spectroscopy technique to hair tissue mineral analysis［J］. Applied Optics, 2003, 42(30): 6133-6137.

[168] 涂彩, 袁心强. 应用激光诱导离解光谱自由定标法测定黄金首饰成分初探［J］. 宝石和宝石学杂志, 2011, 13(4): 1-6.
Tu C, Yuan X Q. A tentative analysis of calibration free-laser induced breakdown spectroscopy for quality inspection of gold jewelry ［J］. Journal of Gems & Gemmology, 2011, 13(4): 1-6.

[169] 陈兴龙, 董凤忠, 王琦, 等. 自由定标激光诱导击穿光谱技术在炉渣成分定量分析中的应用［J］. 光谱学与光谱分析, 2011, 31(12): 3289-3293.
Chen X L, Dong F Z, Wang Q, et al. Quantitative analysis of slag by calibration-free laser-induced breakdown spectroscopy ［J］. Spectroscopy and Spectral Analysis, 2011, 31(12): 3289-3293.

[170] Roldán A M, Pisarćík M, Veis M, et al. Calibration-free analysis of a tungsten-based target for diagnostics of relevant fusion materials comparing picosecond and nanosecond LIBS ［J］. Spectrochimica Acta Part B: Atomic Spectroscopy, 2021, 177: 106055.

[171] Miškovičová J, Anguš M, van der Meiden H, et al. Selection of molybdenum lines by quantitative analysis of molybdenum- zirconium-titanium alloy by CF-LIBS for future fusion applications［J］. Fusion Engineering and Design, 2020, 153: 111488.

[172] Hu Z L, Chen F, Zhang D, et al. A method for improving the accuracy of calibration-free laser-induced breakdown spectroscopy by exploiting self-absorption ［J］. Analytica Chimica Acta, 2021, 1183: 339008.

[173] Death D L, Cunningham A P, Pollard L J. Multi-element analysis of iron ore pellets by laser-induced breakdown spectroscopy and principal components regression［J］. Spectrochimica Acta Part B: Atomic Spectroscopy, 2008, 63(7): 763-769.

[174] Death D L, Cunningham A P, Pollard L J. Multi-element and mineralogical analysis of mineral ores using laser induced breakdown spectroscopy and chemometric analysis［J］. Spectrochimica Acta Part B: Atomic Spectroscopy, 2009, 64(10): 1048-1058.

[175] Yaroshchyk P, Death D L, Spencer S J. Comparison of principal components regression, partial least squares regression, multi-block partial least squares regression, and serial partial least squares regression algorithms for the analysis of Fe in iron ore using LIBS［J］. Journal of Analytical

Atomic Spectrometry, 2012, 27(1): 92-98.

[176] Yaroshchyk P, Death D L, Spencer S J. Quantitative measurements of loss on ignition in iron ore using laser-induced breakdown spectroscopy and partial least squares regression analysis[J]. Applied Spectroscopy, 2010, 64(12): 1335-1341.

[177] 孙兰香, 于海斌, 丛智博, 等. 激光诱导击穿光谱技术结合神经网络定量分析钢中的 Mn 和 Si[J]. 光学学报, 2010, 30(9): 2757-2765.
Sun L X, Yu H B, Cong Z B, et al. Quantitative analysis of Mn and Si of steels by laser-induced breakdown spectroscopy combined with neural networks[J]. Acta Optica Sinica, 2010, 30(9): 2757-2765.

[178] Moncayo S, Manzoor S, Rosales J D, et al. Qualitative and quantitative analysis of milk for the detection of adulteration by laser induced breakdown spectroscopy (LIBS)[J]. Food Chemistry, 2017, 232: 322-328.

[179] Vaniman D, Dyar M D, Wiens R, et al. Ceramic ChemCam calibration targets on Mars science laboratory[J]. Space Science Reviews, 2012, 170 (1/2/3/4): 229-255.

[180] Melikechi N, Mezzacappa A, Cousin A, et al. Correcting for variable laser-target distances of laser-induced breakdown spectroscopy measurements with ChemCam using emission lines of Martian dust spectra[J]. Spectrochimica Acta Part B: Atomic Spectroscopy, 2014, 96: 51-60.

[181] Meslin P Y, Gasnault O, Forni O, et al. Soil diversity and hydration as observed by ChemCam at Gale crater, Mars[J]. Science, 2013, 341(6153): 1238670.

[182] Maurice S, Clegg S M, Wiens R C, et al. ChemCam activities and discoveries during the nominal mission of the Mars Science Laboratory in Gale crater, Mars[J]. Journal of Analytical Atomic Spectrometry, 2016, 31(4): 863-889.

[183] Wiens R C, Maurice S, Robinson S H, et al. The SuperCam instrument suite on the NASA Mars 2020 rover: body unit and combined system tests[J]. Space Science Reviews, 2021, 217(1): 4.

[184] Wan X, Li C, Wang H, et al. Design, function, and implementation of China's first LIBS instrument (MarSCoDe) on the Zhurong Mars rover [J]. Atomic Spectroscopy, 2021, 42(5): 294-298.

[185] Wan X, Yuan R J, Wang H P, et al. Elastic particle swarm optimization for MarSCoDe spectral calibration on Tianwen-1 Mars rover[J]. Analytical Chemistry, 2021, 93(22): 7970-7977.

[186] Xu W M, Liu X F, Yan Z X, et al. The MarSCoDe instrument suite on the Mars rover of China's Tianwen-1 mission[J]. Space Science Reviews, 2021, 217(5): 1-58.

[187] Fabre C. Advances in Laser-induced breakdown spectroscopy analysis for geology: a critical review [J]. Spectrochimica Acta Part B: Atomic Spectroscopy, 2020, 166: 105799.

[188] Harmon R S, Senesi G S. Laser-induced breakdown spectroscopy-a geochemical tool for the 21st century [J]. Applied Geochemistry, 2021, 128: 104929.

[189] Kiros A, Lazic V, Gigante G E, et al. Analysis of rock samples collected from rock hewn churches of Lalibela, Ethiopia using laser-induced breakdown spectroscopy[J]. Journal of Archaeological Science, 2013, 40(5): 2570-2578.

[190] Quarles C D, Gonzalez J J, East L J, et al. Fluorine analysis using laser induced breakdown spectroscopy (LIBS) [J]. Journal of Analytical Atomic Spectrometry, 2014, 29(7): 1238-1242.

[191] Rifai K, Laflamme M, Constantin M, et al. Analysis of gold in rock samples using laser-induced breakdown spectroscopy: matrix and heterogeneity effects[J]. Spectrochimica Acta Part B: Atomic Spectroscopy, 2017, 134: 33-41.

[192] 杨志强, 李光泉, 佘明军. 基于激光诱导击穿光谱的岩屑岩性在线识别试验研究[J]. 石油钻探技术, 2019(4): 122-126.
Yang Z Q, Li G Q, She M J. Test research of online identification of cuttings lithology by LIBS technology [J]. Petroleum Drilling Techniques, 2019(4): 122-126.

[193] 佘明军, 李油建, 李胜利, 等. 激光诱导击穿光谱自动识别泥岩颜色实验分析[J]. 录井工程, 2015, 26(1): 5-8, 84.
She M J, Li Y J, Li S L, et al. Automatic identification of mudstone color using laser-induced breakdown spectroscopy (LIBS) experiment[J]. Mud Logging Engineering, 2015, 26(1): 5-8, 84.

[194] Tian Y, Wang Z N, Han X S, et al. Comparative investigation of partial least squares discriminant analysis and support vector machines for geological cuttings identification using laser-induced breakdown spectroscopy [J]. Spectrochimica Acta Part B: Atomic Spectroscopy, 2014, 102: 52-57.

[195] 王超, 张伟刚, 阎治全. 激光诱导击穿光谱技术对火成岩岩性的高精度识别[J]. 光谱学与光谱分析, 2015, 35(9): 2463-2468.
Wang C, Zhang W G, Yan Z Q. High precision identification of igneous rock lithology by laser induced breakdown spectroscopy[J]. Spectroscopy and Spectral Analysis, 2015, 35(9): 2463-2468.

［196］ Li Q Z, Zhang W, Tang Z Y, et al. Determination of uranium in ores using laser-induced breakdown spectroscopy combined with laser-induced fluorescence［J］. Journal of Analytical Atomic Spectrometry, 2020, 35(3): 626-631.

［197］ 邱苏玲, 李安, 王宪双, 等. 基于激光诱导击穿光谱的矿石中铁含量的高准确度定量分析［J］. 中国激光, 2021, 48(16): 1611002.
Qiu S L, Li A, Wang X S, et al. High-accuracy quantitatively analysis of iron content in mineral based on laser-induced breakdown spectroscopy［J］. Chinese Journal of Lasers, 2021, 48(16): 1611002.

［198］ Fabre C, Devismes D, Moncayo S, et al. Elemental imaging by laser-induced breakdown spectroscopy for the geological characterization of minerals［J］. Journal of Analytical Atomic Spectrometry, 2018, 33(8): 1345-1353.

［199］ Kuhn K, Meima J A, Rammlmair D, et al. Chemical mapping of mine waste drill cores with laser-induced breakdown spectroscopy (LIBS) and energy dispersive X-ray fluorescence (EDXRF) for mineral resource exploration［J］. Journal of Geochemical Exploration, 2016, 161: 72-84.

［200］ Gaft M, Raichlin Y, Pelascini F, et al. Imaging rare-earth elements in minerals by laser-induced plasma spectroscopy: molecular emission and plasma-induced luminescence［J］. Spectrochimica Acta Part B: Atomic Spectroscopy, 2019, 151: 12-19.

［201］ Sweetapple M T, Tassios S. Laser-induced breakdown spectroscopy (LIBS) as a tool for *in situ* mapping and textural interpretation of lithium in pegmatite minerals［J］. American Mineralogist, 2015, 100(10): 2141-2151.

［202］ El Haddad J, de Lima Filho E S, Vanier F, et al. Multiphase mineral identification and quantification by laser-induced breakdown spectroscopy［J］. Minerals Engineering, 2019, 134: 281-290.

［203］ Yan C H, Qi J, Ma J X, et al. Determination of carbon and sulfur content in coal by laser induced breakdown spectroscopy combined with kernel-based extreme learning machine［J］. Chemometrics and Intelligent Laboratory Systems, 2017, 167: 226-231.

［204］ Li S S, Dong M R, Luo F S, et al. Experimental investigation of combustion characteristics and NO_x formation of coal particles using laser induced breakdown spectroscopy［J］. Journal of the Energy Institute, 2020, 93(1): 52-61.

［205］ Stipe C B, Miller A L, Brown J, et al. Evaluation of laser-induced breakdown spectroscopy (LIBS) for measurement of silica on filter samples of coal dust［J］. Applied Spectroscopy, 2012, 66(11): 1286-1293.

［206］ Rong K, Wang Z Z, Hu R M, et al. Experimental study on mercury content in flue gas of coal-fired units based on laser-induced breakdown spectroscopy［J］. Plasma Science and Technology, 2020, 22(7): 074010.

［207］ 余亮英, 陆继东, 陈文, 等. 用激光感生击穿光谱对大气进行定量分析［J］. 应用光学, 2006, 27(2): 147-151.
Yu L Y, Lu J D, Chen W, et al. Quantitative analysis of atmosphere by laser-induced breakdown spectroscopy［J］. Journal of Applied Optics, 2006, 27(2): 147-151.

［208］ Capitelli F, Colao F, Provenzano M R, et al. Determination of heavy metals in soils by laser induced breakdown spectroscopy［J］. Geoderma, 2002, 106(1/2): 45-62.

［209］ Santos D, Jr, Nunes L C, Trevizan L C, et al. Evaluation of laser induced breakdown spectroscopy for cadmium determination in soils［J］. Spectrochimica Acta Part B: Atomic Spectroscopy, 2009, 64(10): 1073-1078.

［210］ Srungaram P K, Ayyalasomayajula K K, Yu-Yueh F, et al. Comparison of laser induced breakdown spectroscopy and spark induced breakdown spectroscopy for determination of mercury in soils［J］. Spectrochimica Acta Part B: Atomic Spectroscopy, 2013, 87: 108-113.

［211］ 许洪光, 管士成, 傅院霞, 等. 土壤中微量重金属元素 Pb 的激光诱导击穿谱［J］. 中国激光, 2007, 34(4): 577-581.
Xu H G, Guan S C, Fu Y X, et al. Laser induced breakdown spectroscopy of the trace metal element Pb in soil［J］. Chinese Journal of Lasers, 2007, 34(4): 577-581.

［212］ 王建伟, 张娜珍, 侯可勇, 等. LIBS 技术在土壤重金属污染快速测量中的应用［J］. 化学进展, 2008, 20(S2): 1165-1171.
Wang J W, Zhang N Z, Hou K Y, et al. Application of LIBS technology to the rapid measure of heavy metal contamination in soils［J］. Progress in Chemistry, 2008, 20(S2): 1165-1171.

［213］ 刘林美, 林兆祥, 李捷, 等. 云台山地质的激光诱导击穿光谱研究［J］. 应用激光, 2008, 28(5): 386-389.
Liu L M, Lin Z X, Li J, et al. Analysis of the Yuntaishan geology by laser-induced breakdown spectroscopy［J］. Applied Laser, 2008, 28(5): 386-389.

［214］ 鲁翠萍，刘文清，赵南京，等. 土壤重金属铬元素的激光诱导击穿光谱定量分析研究［J］. 物理学报，2011，60(4)：395-399.
Lu C P, Liu W Q, Zhao N J, et al. Quantitative analysis of chrome in soil samples using laser-induced breakdown spectroscopy［J］. Acta Physica Sinica, 2011, 60(4): 395-399.

［215］ 潘爱民，刘林美，林兆祥. 土壤中 Cd 元素的激光击穿光谱检测研究［J］. 应用激光，2012，32(2)：124-127.
Pan A M, Liu L M, Lin Z X. Analysis of the Cd element in soil by laser-induced breakdown spectroscopy［J］. Applied Laser, 2012, 32(2): 124-127.

［216］ 陈添兵，姚明印，刘木华，等. 用激光诱导击穿光谱技术定量分析土壤中 Ba 和 Sr［J］. 光谱学与光谱分析，2012，32(6)：1658-1661.
Chen T B, Yao M Y, Liu M H, et al. Quantitative analysis of Ba and Sr in soil using laser-induced breakdown spectroscopy［J］. Spectroscopy and Spectral Analysis, 2012, 32(6): 1658-1661.

［217］ Yi R X, Yang X Y, Zhou R, et al. Determination of trace available heavy metals in soil using laser-induced breakdown spectroscopy assisted with phase transformation method［J］. Analytical Chemistry, 2018, 90(11): 7080-7085.

［218］ Gao P Y, Yang P, Zhou R, et al. Determination of antimony in soil using laser-induced breakdown spectroscopy assisted with laser-induced fluorescence［J］. Applied Optics, 2018, 57(30): 8942-8946.

［219］ Rai V N, Yueh F Y, Singh J P. Study of laser-induced breakdown emission from liquid under double-pulse excitation［J］. Applied Optics, 2003, 42(12): 2094-2101.

［220］ Rai N K, Rai A K, Kumar A, et al. Detection sensitivity of laser-induced breakdown spectroscopy for Cr II in liquid samples［J］. Applied Optics, 2008, 47(31): G105-G111.

［221］ Koch S, Court R, Garen W, et al. Detection of manganese in solution in cavitation bubbles using laser induced breakdown spectroscopy［J］. Spectrochimica Acta Part B: Atomic Spectroscopy, 2005, 60(7/8): 1230-1235.

［222］ Matsumoto A, Tamura A, Koda R, et al. On-site quantitative elemental analysis of metal ions in aqueous solutions by underwater laser-induced breakdown spectroscopy combined with electrodeposition under controlled potential［J］. Analytical Chemistry, 2015, 87(3): 1655-1661.

［223］ Cheung N H, Yeung E S. Single-shot elemental analysis of liquids based on laser vaporization at fluences below breakdown ［J］. Applied Spectroscopy, 1993, 47(7): 882-886.

［224］ Feng Y, Yang J J, Fan J M, et al. Investigation of laser-induced breakdown spectroscopy of a liquid jet［J］. Applied Optics, 2010, 49(13): C70-C74.

［225］ Huang J S, Ke C B, Huang L S, et al. The correlation between ion production and emission intensity in the laser-induced breakdown spectroscopy of liquid droplets［J］. Spectrochimica Acta Part B: Atomic Spectroscopy, 2002, 57(1): 35-48.

［226］ Zhang D C, Hu Z Q, Su Y B, et al. Simple method for liquid analysis by laser-induced breakdown spectroscopy (LIBS)［J］. Optics Express, 2018, 26(14): 18794-18802.

［227］ Yang X Y, Li X Y, Cui Z F, et al. Analytical-performance improvement of aqueous solution by chemical replacement combined with surface-enhanced laser-induced breakdown spectroscopy［J］. Applied Optics, 2018, 57(25): 7135-7139.

［228］ Gondal M A, Habibullah Y B, Baig U, et al. Direct spectral analysis of tea samples using 266 nm UV pulsed laser-induced breakdown spectroscopy and cross validation of LIBS results with ICP-MS［J］. Talanta, 2016, 152: 341-352.

［229］ Cho H H, Kim Y J, Jo Y S, et al. Application of laser-induced breakdown spectrometry for direct determination of trace elements in starch-based flours ［ J ］. Journal of Analytical Atomic Spectrometry, 2001, 16(6): 622-627.

［230］ 何秀文，黄林，刘木华，等. 激光诱导击穿光谱对大米中镉元素的检测分析［J］. 应用激光，2014，34(1)：72-75.
He X W, Huang L, Liu M H, et al. Determination of Cd in rice by laser-induced breakdown spectroscopy［J］. Applied Laser, 2014, 34(1): 72-75.

［231］ Peng J Y, He Y, Ye L H, et al. Moisture influence reducing method for heavy metals detection in plant materials using laser-induced breakdown spectroscopy: a case study for chromium content detection in rice leaves［J］. Analytical Chemistry, 2017, 89(14): 7593-7600.

［232］ Liu F, Ye L H, Peng J Y, et al. Fast detection of copper content in rice by laser-induced breakdown spectroscopy with uni- and multivariate analysis［J］. Sensors, 2018, 18(3): 705.

［233］ 杨晖，黄林，刘木华，等. 双光束激光诱导击穿光谱提高污染大米中镉元素检测灵敏度实验［J］. 激光与光电子学进展，2016，53(5)：053005.
Yang H, Huang L, Liu M H, et al. Improvement

of analytical sensitivity on detecting Cd residue in rice by dual pulse laser induced breakdown spectroscopy［J］. Laser & Optoelectronics Progress, 2016, 53(5): 053005.

[234] 胡慧琴, 徐雪红, 黄林, 等. 微波辅助激光诱导击穿光谱增强大米中 Cd 发射强度的研究[J]. 光谱学与光谱分析, 2016, 36(4): 1180-1185.
Hu H Q, Xu X H, Huang L, et al. Study on the enhancement intensity of Cd in rice with microwave-assisted laser-induced breakdown spectroscopy［J］. Spectroscopy and Spectral Analysis, 2016, 36(4): 1180-1185.

[235] Kim G, Kwak J, Choi J, et al. Detection of nutrient elements and contamination by pesticides in spinach and rice samples using laser-induced breakdown spectroscopy (LIBS)［J］. Journal of Agricultural and Food Chemistry, 2012, 60(3): 718-724.

[236] 饶刚福, 黄林, 刘木华, 等. 基于激光诱导击穿光谱的微生物种类鉴别研究[J]. 分析化学, 2018, 46(7): 1122-1128.
Rao G F, Huang L, Liu M H, et al. Discrimination of microbe species by laser induced breakdown spectroscopy［J］. Chinese Journal of Analytical Chemistry, 2018, 46(7): 1122-1128.

[237] Prochazka D, Mazura M, Samek O, et al. Combination of laser-induced breakdown spectroscopy and Raman spectroscopy for multivariate classification of bacteria［J］. Spectrochimica Acta Part B: Atomic Spectroscopy, 2018, 139: 6-12.

[238] Bilge G, Velioglu H M, Sezer B, et al. Identification of meat species by using laser-induced breakdown spectroscopy［J］. Meat Science, 2016, 119: 118-122.

[239] Yueh F Y, Zheng H B, Singh J P, et al. Preliminary evaluation of laser-induced breakdown spectroscopy for tissue classification［J］. Spectrochimica Acta Part B: Atomic Spectroscopy, 2009, 64(10): 1059-1067.

[240] 朱毅宁, 杨平, 杨新艳, 等. 支持向量机结合主成分分析辅助激光诱导击穿光谱技术识别鲜肉品种［J］. 分析化学, 2017, 45(3): 336-341.
Zhu Y N, Yang P, Yang X Y, et al. Classification of fresh meat species using laser-induced breakdown spectroscopy with support vector machine and principal component analysis[J]. Chinese Journal of Analytical Chemistry, 2017, 45(3): 336-341.

[241] 陈添兵, 刘木华, 黄林, 等. 不同光谱预处理对激光诱导击穿光谱检测猪肉中铅含量的影响[J]. 分析化学, 2016, 44(7): 1029-1034.
Chen T B, Liu M H, Huang L, et al. Effects of

different pretreatment method on laser-induced breakdown spectroscopy measurement of Pb in pork [J]. Chinese Journal of Analytical Chemistry, 2016, 44(7): 1029-1034.

[242] 吴鼎, 海然, 刘平, 等. 基于激光诱导击穿光谱地沟油鉴别的初步探究［J］. 科学通报, 2014, 59(21): 2071-2076.
Wu D, Hai R, Liu P, et al. Preliminary study of identifying trench oil based on laser-induced breakdown spectroscopy［J］. Chinese Science Bulletin, 2014, 59(21): 2071-2076.

[243] 朱泉水, 郝仕国, 罗宁宁, 等. 基于激光诱导荧光的植物油掺假检测与量化分析［J］. 中国激光, 2019, 46(12): 1211002.
Zhu Q S, Hao S G, Luo N N, et al. Detection and quantification of vegetable oil adulteration based on laser-induced fluorescence spectroscopy[J]. Chinese Journal of Lasers, 2019, 46(12): 1211002.

[244] Caceres J O, Moncayo S, Rosales J D, et al. Application of laser-induced breakdown spectroscopy (LIBS) and neural networks to olive oils analysis ［J］. Applied Spectroscopy, 2013, 67(9): 1064-1072.

[245] Gazeli O, Bellou E, Stefas D, et al. Laser-based classification of olive oils assisted by machine learning[J]. Food Chemistry, 2020, 302: 125329.

[246] Bellou E, Gyftokostas N, Stefas D, et al. Laser-induced breakdown spectroscopy assisted by machine learning for olive oils classification: the effect of the experimental parameters［J］. Spectrochimica Acta Part B: Atomic Spectroscopy, 2020, 163: 105746.

[247] Gyftokostas N, Stefas D, Kokkinos V, et al. Laser-induced breakdown spectroscopy coupled with machine learning as a tool for olive oil authenticity and geographic discrimination［J］. Scientific Reports, 2021, 11: 5360.

[248] Stefas D, Gyftokostas N, Kourelias P, et al. Discrimination of olive oils based on the olive cultivar origin by machine learning employing the fusion of emission and absorption spectroscopic data [J]. Food Control, 2021, 130: 108318.

[249] Vrenegor J, Noll R, Sturm V. Investigation of matrix effects in laser-induced breakdown spectroscopy plasmas of high-alloy steel for matrix and minor elements［J］. Spectrochimica Acta Part B: Atomic Spectroscopy, 2005, 60(7/8): 1083-1091.

[250] Mermet J M, Mauchien P, Lacour J L. Processing of shot-to-shot raw data to improve precision in laser-induced breakdown spectrometry microprobe ［J］. Spectrochimica Acta Part B: Atomic

Spectroscopy, 2008, 63(10): 999-1005.

[251] Sturm V, Fleige R, de Kanter M, et al. Laser-induced breakdown spectroscopy for 24/7 automatic liquid slag analysis at a steel works[J]. Analytical Chemistry, 2014, 86(19): 9687-9692.

[252] Tsai S J J, Chen S Y, Chung Y S, et al. Spatially resolved, laser-induced breakdown spectroscopy, development, and application for the analysis of Al and Si in nickel-based alloys [J]. Analytical Chemistry, 2006, 78(21): 7432-7439.

[253] Zhu D H, Wang X, Ni X W, et al. Determination of aluminum in nickel-based superalloys by using laser-induced breakdown spectroscopy[J]. Plasma Science and Technology, 2011, 13(4): 486-489.

[254] Gupta G P, Suri B M, Verma A, et al. Quantitative elemental analysis of nickel alloys using calibration-based laser-induced breakdown spectroscopy [J]. Journal of Alloys and Compounds, 2011, 509(9): 3740-3745.

[255] Kim T H, Lee D H, Kim D, et al. Analysis of oxidation behavior of Ni-base superalloys by laser-induced breakdown spectroscopy [J]. Journal of Analytical Atomic Spectrometry, 2012, 27(9): 1525-1531.

[256] Shen M, Li C M, Na D, et al. Determination of yttrium in titanium alloys using laser-induced breakdown spectroscopy assisted with laser-induced fluorescence [J]. Journal of Analytical Atomic Spectrometry, 2018, 33(4): 658-662.

[257] Busser B, Moncayo S, Coll J L, et al. Elemental imaging using laser-induced breakdown spectroscopy: a new and promising approach for biological and medical applications[J]. Coordination Chemistry Reviews, 2018, 358: 70-79.

[258] Kumar A, Yueh F Y, Singh J P, et al. Characterization of malignant tissue cells by laser-induced breakdown spectroscopy [J]. Applied Optics, 2004, 43(28): 5399-5403.

[259] Han J H, Moon Y, Lee J J, et al. Differentiation of cutaneous melanoma from surrounding skin using laser-induced breakdown spectroscopy [J]. Biomedical Optics Express, 2015, 7(1): 57-66.

[260] Chen X, Li X H, Yu X, et al. Diagnosis of human malignancies using laser-induced breakdown spectroscopy in combination with chemometric methods[J]. Spectrochimica Acta Part B: Atomic Spectroscopy, 2018, 139: 63-69.

[261] Markushin Y, Sivakumar P, Connolly D, et al. Tag-femtosecond laser-induced breakdown spectroscopy for the sensitive detection of cancer antigen 125 in blood plasma [J]. Analytical and Bioanalytical Chemistry, 2015, 407(7): 1849-1855.

[262] Samek O, Beddows D C S, Telle H H, et al. Quantitative laser-induced breakdown spectroscopy analysis of calcified tissue samples [J]. Spectrochimica Acta Part B: Atomic Spectroscopy, 2001, 56(6): 865-875.

[263] Bilmes G M, Freisztav C, Schinca D, et al. Cleaning and characterization of objects of cultural value by laser ablation[J]. Proceedings of SPIE, 2005, 5857: 585704.

[264] Hamzaoui S, Khleifia R, Jaïdane N, et al. Quantitative analysis of pathological nails using laser-induced breakdown spectroscopy (LIBS) technique[J]. Lasers in Medical Science, 2011, 26(1): 79-83.

[265] Ng C W, Cheung N H. Detection of sodium and potassium in single human red blood cells by 193-nm laser ablative sampling: a feasibility demonstration [J]. Analytical Chemistry, 2000, 72(1): 247-250.

Laser-Induced Breakdown Spectroscopy and Its Application

Li Xiangyou[*], Liu Ke, Zhou Ran, Zhang Wen

Wuhan National Laboratory for Optoelectronics, Huazhong University of Science and Technology, Wuhan 430074, Hubei, China

Abstract

Significance　　The physical and chemical properties of materials are determined by their element compositions and contents. How to obtain the compositions and content information of materials quickly, accurately, and at low cost has always been the research direction of scholars. The existing methods for the analysis of elements in the materials can be divided into the chemical methods and the instrumental methods. Based on the law of chemical reactions, the chemical methods carry out the qualitative and quantitative systematic analysis on the chemical compositions of

samples, including the gravimetric method, the volumetric method, and the colorimetric method. In contrast, the instrumental methods directly obtain the physical and chemical information of the unknown samples through the analytical instruments, such as the inductively coupled plasma mass spectrometry, the Raman spectrum, the near-infrared spectrum, the X-ray spectrometry, and the atomic absorption spectrometry. The above-mentioned methods can obtain the categories and composition information of the samples with high sensitivity and accuracy, but they present complex operation, high cost, and low efficiency. However, with the continuous expansion of application fields, there is a high demand for the analysis technologies. Looking for a newer, faster, and more adaptive detection technology has become a research hotspot.

Laser induced breakdown spectroscopy (LIBS) is an element analysis technology, which uses a laser as the excitation source to ablate the sample and produce plasma. The emission spectrum of the plasma is then detected by a spectrometer to obtain the element category and the content information of the sample to be measured. Compared with other analytical technologies, the LIBS technology has the unique advantages of simultaneous detection of multiple elements, simple structure, fast detection speed, and being not affected by sample morphology. It shows great application prospects in many fields. Based on this, the mechanism, device types, basic research progress, and applications of LIBS are summarized.

Progress　The plasma characteristics and self-absorption effect of the LIBS instruments raise the most concerns. By studying the relevant characteristics of plasma, it is helpful to understand the generation mechanism of laser-induced plasma and solve the relevant problems encountered in the LIBS analysis. The self-absorption infulences the linear relationship between the original plasma emission spectral intensity and the concentration of related elements, and thus it reduces the accuracy of a quantitative analysis. To satisfy different analytical requirements, variable types of LIBS instruments are developed, including an LIBS in the laboratory (Fig. 3), a stand-off LIBS (Fig. 4), an on-line LIBS (Fig. 5), and a portable LIBS (Fig. 6). The LIBS in the laboratory has higher sensitivity and reproducibility, which is often used in the study of mechanism and exploratory applications. The stand-off LIBS can realize an *in-situ* detection of dangerous samples under harsh conditions on the premise of ensuring personnel safety. With the unique advantages of *in-situ* detection, real-time, fast, and no complex sample pretreatment, the on-line LIBS can quickly process numerous samples on the production line. The portable LIBS has the advantages of small volume, light weight, and convenient use, which has better applicability in industrial fields with harsh conditions.

To improve the analytical performance of the LIBS technology, the signal enhancement methods and the methods for the qualitative and quantitative analysis have become the focus study. The signal enhancement methods mainly contain surface enhancement methods (Fig. 7), inert-gas protection enhancement methods (Fig. 9), confinement enhancement methods (Fig. 10), and double-pulse enhancement methods (Fig. 11). The surface enhancement method ablate the substrate and the sample to be measured at the same time. The high-temperature plasma generated by the substrate heats the sample which can improve the temperature and electron number density of the sample plasma. Using inert gas as ambient gas can prolong the life of luminous atoms in plasma and avoid the light signal from being absorbed by air. Confinement enhancement uses the confinement cavity or magnetic field to affect the external and internal conditions of the plasma and confine the plasma to achieve signal enhancement with the advantages of simplicity, economy, and high feasibility. The double-pulse technology uses the second laser pulse to excite and heat the plasma again, which can greatly increase the temperature of the plasma and enhance the spectral intensity. Various methods are carried out for the qualitative and quantitative analysis, including material identification, element detection, and quantitative analysis.

Conclusions and Prospects　With the specific advantages of the LIBS technology and the development of above-mentioned methods, the LIBS technology has been successfully used in various fields, including space exploration (Fig. 14), geological prospection (Fig. 15), pollution monitoring (Fig. 16), food safety (Fig. 17), industrial metallurgy (Fig. 18), and biomedicine (Fig. 19). The rapid identification of sample category is the focus of current research, and good analytical results have been obtained. However, due to the change of experimental environments, surface dirt of samples, and the diversity of manufacturing processes and additives, the prediction accuracy of the LIBS technology for real samples is still low. Outlier screening, variable selection, scale transformation, and other spectral preprocessing methods, as well as the improvement and integration of algorithms, are effective ways to solve this problem. Due to the matrix effect, laser energy fluctuation, spectrometer resolution difference, detection environment limitation, and other reasons, the LIBS technology has a large deviation in the prediction of element contents in materials. Optimizing the LIBS instrument platform, studying the signal

enhancement methods, and improving the analysis methods are the effective methods to improve the prediction accuracy of the quantitative analysis.

The matrix effect is the most critical problem that limits the wide application of the LIBS technology. With the continuous development of the LIBS instruments and the corresponding components, this problem can be effectively solved, but it will take a long time. The improvement of the analytical chemistry method will be an effective way to improve the application performance of the LIBS technology. In order to realize the rapid and sensitive detection of massive materials, the development of an on-line LIBS device will be the development trend in the future.